Ages and stratigraphical architecture of late Miocene deposits in the Lorca Basin (Betics, SE Spain): New insights for the salinity crisis in marginal basins

Cédric Carpentier, Emmanuelle Vennin, Jean-Marie Rouchy, Jean-Jacques Cornée, Mihaela Melinte-Dobrinescu, Christian Hibsch, Nicolas Olivier, Antonio Caruso, Danièle Bartier

Ages and stratigraphical architecture of late Miocene deposits in the Lorca Basin (Betics, SE Spain): New insights for the salinity crisis in marginal basins.

Cédric Carpentier , Emmanuelle Vennin , Jean-Marie Rouchy , Jean-Jacques Cornée ,
Mihaela Melinte-Dobrinescu, Christian Hibsch, Nicolas Olivier, Antonio Caruso, Danièle Bartier

Keywords-Tortonian Messinian Salinity crisis Stratigraphy Base-level fluctuations Lorca Basin BeticsSpain

Abstract-
Unlike most Neogene basins of the Betic Cordillera where the Salinity Crisis is dated to the Messinian, a contradictory Tortonian dating was proposed for evaporites of the Lorca Basin. As a consequence, complex structural models have been proposed in the literature to explain this discrepancy in the timing of evaporites. In order to integrate the Lorca Basin into the geological context of the western Mediterranean domain during the Late Miocene, new sedimentological and stratigraphical studies coupled with new dating were performed, which allow us to propose a Messinian age for both diatomite-bearing deposits and evaporites of the Lorca Basin. These new ages challenge the idea of a Tortonian salinity crisis in the Lorca Basin. Three main events of base-level drop were evidenced during the Messinian. Each event is correlated with successive steps of basin restriction. Shallow salina evaporites were deposited after a base-level fall during the Messinian before a final base-level drop, which led to the entire exposure of the basin. This last exposure is interpreted as coeval with the deposition of first evaporites and halite in the deep Mediterranean basins. The reflooding which allowed the deposition of brackish deposits and a short-lived marine incursion occurred at the end of the Messinian. Base-level drops occurred during eustatic falls amplified by the gradual uplift of the Betic Cordillera. The exhumation of the Tercia ridge along the strike-slip Alhama de Murcia fault system during the Messinian probably favoured the gradual restriction of the basin. A discussion on correlations of main unconformities between several Neogene basins of the Betics is proposed, suggesting a similar structural evolution at the regional scale.

1. Introduction

Since the pioneer desiccated deep-basin model of Hsü et al. (1973) and Hsü et al. (1973) the Messinian salinity crisis (MSC) has been the subject of numerous publications. Several authors subdivided deep and marginal evaporites in lower and upper units (e.g., Butler et al., 1995; Rouchy and Caruso, 2006; Roveri et al., 2008, 2014a; Ryan, 2009; Manzi et al., 2013). Nevertheless, the relative timing of evaporite units in marginal basins compared with evaporites of the central Mediterranean Sea is intensely debated (e.g., Clauzon et al., 1996; Riding et al., 1998; Martin et al., 1999; Rouchy and Caruso, 2006; Roveri et al., 2008, 2014a; Orszag-Sperber et al., 2009; Cornée et al., 2016;

Karakitsios et al., 2017; Merzeraud et al., 2019). Indeed, some authors consider that marginal evaporites were deposited before the main relative sea-level drop, which led to the deposition of central Mediterranean evaporites (Clauzon et al., 1996; Maillard et al., 2006; Lugli et al., 2015). This interpretation argues for a synchronous onset of the salinity crisis at the basin scale (Gautier et al., 1994; Krijgsman et al., 1999). Recently, Manzi et al. (2013) and Roveri et al. (2014a, 2014b) postulated the equivalence of the marginal evaporites with the euxinic shales in the deeper Mediterranean. In this case, marginal evaporites rest conformably on diatomite-rich shales (Tripoli Formation or Abad Formation) and are topped by a major surface of incision and subaerial exposure. Other authors such as Riding et al. (1998) or Braga et al. (2006) proposed that only few or no evaporites were deposited in marginal basins prior to the major relative sea-level drop responsible of deposition of central Mediterranean evaporites. They consider that the evaporites in marginal basins (e.g., gypsum of the Sorbas Basin) are younger than deep Mediterranean evaporites and were deposited during the subsequent relative sea-level rise.

In most Neogene basins of the Betic Cordillera such as Sorbas, Nijar, Bajo-Segura, and Murcia-Cartagena basins, gypsum deposits are considered as Messinian in age (e.g., Martin and Braga, 1996; Fortuin and Krijgsman, 2003; Soria et al., 2005, 2008; Braga et al., 2006; Fortuin and Dabrio, 2008). Sedimentary facies similar to those known in other basins of the internal Betics (e.g., Sorbas and Nijar basins) are present in the Lorca Basin. They consist of Porites-rich carbonates, diatomitebearing marls, and gypsum. However their ages are debated. In the Lorca Basin and the neighbouring Fortuna Basin a Messinian age was initially proposed for diatomite-rich marls and gypsum units (Guillen Mondejar et al., 1995; Dinarès-Turell et al., 1997; Rouchy et al., 1998; Wrobel and Michalzik, 1999; Playà et al., 2000). This Messinian age for the evaporites and underlying diatomites of the Lorca Basin was again suggessted by Saelen et al. (2016) on the basis of strontium isotopes. The Tale Gypsum of the Fortuna Basin was also considered as Early Messinian in age by Lancis et al. (2010). Krijgsman et al. (2000, 2006) and Tent-Manclus et al. (2008) challenged this dating and proposed a Tortonian age for evaporites of these two basins. More recently, this Tortonian age for evaporites of the Lorca Basin was also considered by Corbi et al. (2012) and Garcia-Veigas et al. (2019). Consequently, the concept of “Tortonian Salinity Crisis” has been widely adopted and geodynamic models involving differential uplift and subsidence rates between basins along trans-Alboran strike-slip faults were produced to explain diachronous confinements of Neogene basins (Garces et al., 2001; Krijgsman et al., 2006; Rodriguez-Fernandez et al., 2012).

The Lorca Basin is located in the Alboran domain where numerous marginal basins in Spain, Morocco and Algeria can be used to compare the timing of the sedimentary infill. The Lorca Basin constitutes a key area for the reconstruction of the tectonic and stratigraphical history of the salinity crisis in the Betic domain. The basin is located between the Guadix Basin in the external Betic zone, which is devoid of evaporites and where the marine-continental transition occurred during the Tortonian (Soria et al., 1999; Betzler et al., 2006; Pla-Pueyo et al., 2009; Hüsing et al., 2010) and more external basins where Messinian gypsum is present. While the stratigraphical architecture of late Tortonian-Messinian deposits in most the Neogene basins in the Betics has been studied and debated in an abundant literature (e.g., contradictory models of Conesa et al., 1999; Braga et al., 2006; Manzi et al., 2013; Clauzon et al., 2015; Do Couto et al., 2015 in the Sorbas Basin), this is not the case for the Lorca Basin where halite deposits were described in drillings (Orti et al., 1993; Garcia-Veigas et al., 1994, 2019). In addition, new dating approaches are necessary to solve the recurrent problem about the age of the evaporites in the Lorca Basin. Based on new biostratigraphical dating, we propose a correlation between the central and marginal successions in the southwestern part of the basin. Thereafter, a study of the stratigraphical architecture and erosional surfaces between the margins and the centre of the basin based on field observations is illustrated. Finally, the results obtained in the Lorca Basin are compared with neighbouring Neogene basins and discussed within the regional geodynamic and sedimentological framework.

2. Geological framework

The Betic Cordillera is an orogenic complex located in southeastern Spain and oriented ENE-WSW between Cadiz to the southwest and the Cabo de la Nao to the northeast (Fig. 1A). The Betics are part of the Gibraltar arc which includes the Rif Mountains in Morocco and which was formed by the convergence between the Iberian and African plates (Dercourt et al., 1986) (Fig. 1B). To the north, the Guadalquivir Basin corresponds to the flexural foreland basin between the External Betics and the Iberian platform (Cloetingh et al., 1992; de Galdeano and Vera, 1992; Riaza and Martinez del Olmo, 1996; Iribarren et al., 2007).

The External Zone comprises folded and thrusted Mesozoic to Neogene sediments (Vera, 1983; Frizon de Lamotte et al., 1989; Blankenship, 1992; Galindo-Zaldivar et al., 1993). The Internal Betics represent the terrestrial continuation of the Alboran crustal domain (Comas et al., 1992; de Galdeano and Vera, 1992) mainly located offshore between Spain and Morrocco and bounded to the west by the Gibraltar Arc (Iribarren et al., 2007; Platt, 2007). They consist of metamorphic sierras separated by narrow and complex basins filled by Neogene sediments (de Galdeano, 1990; Montenat, 1996; Meijninger and Vissers, 2006) (Fig. 1C). The Lorca Basin displays a rhomboidal shape and is bounded to the southeast by the strike-slip Alhama de Murcia Fault while its northwestern margin impinges on the boundary between the Internal-External Zones (e.g., Guillen Mondejar et al., 1995; Booth-Rea et al., 2002; Martinez-Diaz, 2002) (Fig. 1C). The study area is located on the southwestern margin of the basin where Late Miocene outcrops are well exposed and where synsedimentary normal faults were described in the literature (Guillen Mondejar et al., 1995; Montenat and Ott d'Estevou, 1999; Vennin et al., 2004) (Fig. 2). In the centre of the basin a major NE-SW fault named FCCL (Falla del centro de la Cuenca de Lorca) was envisioned by several authors to explain the differential subsidence between the eastern and western parts of the Lorca Basin during the Late Miocene (Guillen Mondejar et al., 1995; Meijninger and Vissers, 2006).

Because of the frequent occurrence of strike slip faults on their edges, most Neogene basins were first interpreted as pull-apart or “groove-shaped synclines” formed in a transcurrent context active from the Early or Middle Miocene until present (Cloetingh et al., 1992; Montenat and Ott d'Estevou, 1996, 1999; Huibregtse et al., 1998). In contrast, some authors consider that most Neogene basins were formed in an extensional context controlled by high angle normal faults on top of detachments during the collapse of the Alboran domain and the exhumation of metamorphic complexes (Vissers et al., 1995; Chalouan et al., 1997; Booth-Rea et al., 2004; Vazquez et al., 2011; Do Couto et al., 2014, 2016). In this scenario the main NE-SW to N-S strike-slip faults (Carboneras, Palomares, and Alhama de Murcia faults, Fig. 1B) initially acted as normal or transfer faults (Martinez-Martinez et al., 2006; Meijninger and Vissers, 2006; Rodriguez-Fernandez et al., 2012; Giaconia et al., 2014) and were reactivated as strike-slip faults only from the Upper Tortonian or earliest Messinian because of a rotation of the regional stress field (Booth-Rea et al., 2003; Augier et al., 2013).

3. Lithostratigraphical framework

In the western part of the basin, Tortonian sediments unconformably cover Serravalian glauconitic sandstones, marls, and conglomerates of the Soriana Formation (Fm) (Fig. 3). In the souteastern part, slightly metamorphosed Triassic sediments represent the basement. In this area (Castillo de Lorca and Serrata areas) the oldest deposits consist of an alternation of red conglomerates, variegated silty shales, and locally evaporites. These deposits are supposed to be Early Tortonian in age (Montenat, 1996; Wrobel and Michalzik, 1999). They are overlain by calcarenitic and sandy limestones rich in pectinids and Clypeaster sea urchins, which are covered by a thick unit of grey marls corresponding to the Tortonian Marls of Rouchy et al. (1998), or Lower to Upper preevaporitic unit of Wrobel and Michalzik, 1999 dated to the late Tortonian on the basis of foraminifera assemblages (Rouchy et al., 1998; Wrobel and Michalzik, 1999; Krijgsman et al., 2000). Krijgsman et al. (2000) considered these marls as the lateral equivalent of the carbonates of the Parilla and Hondo Fms. On the western margin, the first Tortonian deposits constitute the Parilla Fm that corresponds to the Lower pre-evaporitic unit of Wrobel and Michalzik (1999). The study of foraminifera assemblages allowed these authors to propose a Tortonian age for this formation. Its lower part consists of marine sandstones and shales dated to the Early Tortonian (Vennin et al., 2004) on the basis of planktonic foraminifera. The upper part of the Parilla Fm is characterised by an alternation of Porites or Tarbellastrea-

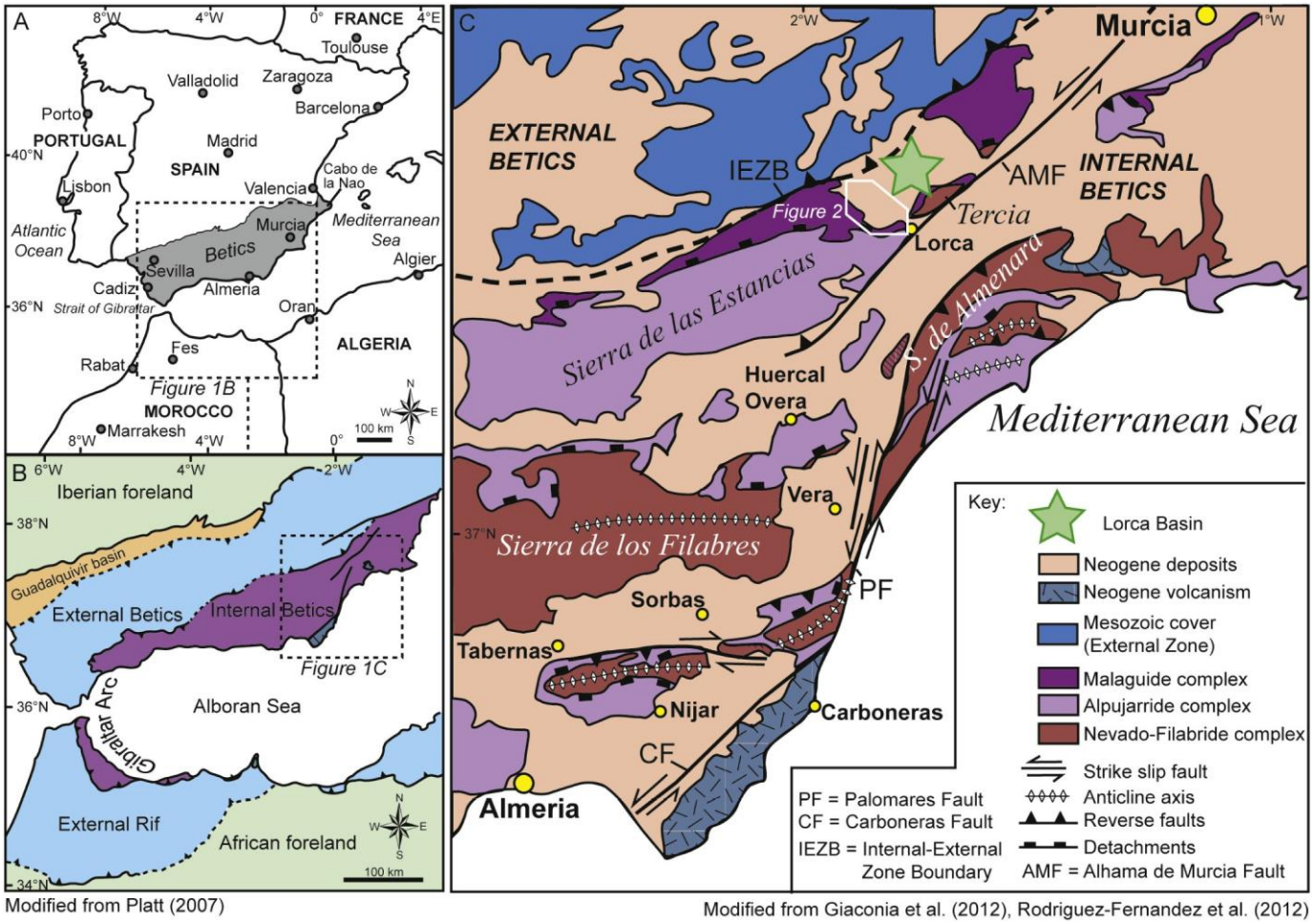

Modified from Platt (2007)

Modified from Giaconia et al. (2012), Rodriguez-Fernandez et al. (2012)

Fig. 1. Location map of the study area. A) Geographical location of the Betic Cordillera; B) Main structural units of the Alboran domain with location of the map in C; C) Geological map of the main Neogene basins in the Internal Betics with location of the Lorca Basin and the study area (Fig. 2).

rich carbonates, red marls rich in large Crassostrea gryphoides (Saelen et al., 2016) with sparse sandstone beds, alluvial conglomerates (Thrana and Talbot, 2006), and grey offshore marls. The Hondo Fm, also named middle pre-evaporitic unit by Wrobel and Michalzik (1999), consists of Tarbellastrea and Porites-rich carbonates.

On the western margin, the upper pre-evaporitic unit of Wrobel and Michalzik (1999) also named Serrata Fm by Vennin et al. (2004) and Thrana and Talbot (2006) consists of an alternation of marine sandstones, conglomerates and coral-rich limestones. A Messinian age was proposed by Wrobel and Michalzik (1999) for the upper preevaporitic unit. A similar age was given by Saelen et al. (2016) on the basis of Sr isotopes. Alternations of red conglomerates and variegated marls constitutes the evaporitic unit and El Prado Fm of Thrana and Talbot (2006) and evaporitic and post-evaporitic units of Wrobel and Michalzik (1999). Wrobel and Michalzik (1999) envisioned a Messinian age for the lower part of the Post-evaporitic unit on the basis of foraminifera assemblages.

In the Serrata area, the evaporites are underlain by the Lower and Upper Tripoli Fms consisting of an alternation of marls, diatomites, dolomites, sandstones, and limestone beds (Upper pre-evaporitic unit of Wrobel and Michalzik (1999)). Rouchy et al. (1998) proposed a Tortonian age for the marls and a Messinian age for the Tripoli Fm based on foraminifera and nannofossils. They located the TortonianMessinian boundary 25 m below the first diatomite bed. Wrobel and Michalzik (1999) established a similar age on the basis of planktonic foraminifera. Corbi et al. (2012) attributed a Tortonian age to the lowermost part of the Lower Tripoli Fm on the basis of the dominance of dextral forms of Neogloboquadrina acostaensis, while Rouchy et al. (1998) placed this event in the Messinian. Krijgsman et al. (2000) also found biostratigraphical markers of the late Tortonian in the Hondo Fm but no Messininan markers in the Tripoli Fm. For these authors, the appearance of Globorotalia miotumida group in the upper part of the Hondo Fm corresponds to one of the short preliminary influxes that occurred in the C4N.2n subchorn during the upper Tortonian and for these reasons they assigned a late Tortonian age to the Tripoli Fm. However, it is important to note that the finding of the G. miotumida group falls within the C4N.2n subchron with an astronomical age of 7.892 Ma, as also described by Hilgen et al. (1995). According to Lirer et al. (2019) this event slightly predates the fist occurrence (FO) of G. suterae which allows to recognise the MMi12b biozone, with an age of 7.80 Ma. The G. miotumida group proposed by Hilgen et al. (1995, 2000a), includes various morphotypes (e.g., G. saphoe, G. mediterranea, G. miotumida sensu stricto (s.s.), G. conoidea, and G. conomiozea s.s.; see Lirer et al., 2019 for more details). According to Hilgen et al. (2000a) the first regular occurrence (FRO) of G. miotumida group allows to recognise the base of the Messinian that falls within the C3Br chron, with an astronomical age of 7.246 Ma (Lourens et al., 2004). On the other hand, the species G. conomiozea s.s. described by Kennett and Srinivasan (1983) is slightly different from G. miotumida both in the height of the throcospire and in the overture and shape of the chambers. As already described by Lirer et al. (2019) "…the FO of G. conomiozea s.s. that was previously adopted to define the Tortonian/Messinian boundary […] occurs 2/3 precessional cycles above the FRO of G. miotumida". Finally, the bioevent described here as G. conomiozea s.s. occurs at the base of the MMi13a biozone into the Messinian within the C3Bn chron (Sprovieri et al., 1996). The dating of Krijgsman et al. (2000) was also based on the absence of typical Messinian nannofossils such as Amaurolithus taxa and Reticulofenestra rotaria and on the absence of Reticulofenestra pseudoumbilicus nannofossils interpreted as the signature of the R. pseudoumbilicus paracme, which extended from 8.8 to 7.1 Ma during the Late Tortonian. In addition to the biostratigraphical dating based on the absence of foraminifera or nannofossils species in diatomites rather than on the occurrence of biostratigraphical markers, the age was mainly constrained on the basis of magnetostratigraphy. Corbi et al. (2012) and Garcia-Veigas et al. (2019) also considered a Tortonian age for the diatom-bearing deposits and overlying evaporites but did not provide new direct biostratigraphical evidences.

The Upper Tripoli Fm is covered by evaporite-rich units named Gypsum unit or Evaporitic unit by Rouchy et al. (1998) or Wrobel and Michalzik (1999), respectively. All these authors proposed a Messinian age for these evaporites, while Krijgsman et al. (2000) considered a Tortonian age. A Tortonian age was also proposed by Garcia-Veigas et al. (2019) on the basis of ages proposed by Corbi et al. (2012) themselves based on ages proposed by Krijgsman et al. (2000). The overlying pink marls and sandstones correspond to the Post-evaporitic unit attributed to the Messinian by Wrobel and Michalzik (1999). However, Rouchy et al. (1998) and Garcia-Veigas et al. (2019) only found reworked foraminifera and non-marine biostratigraphical markers, which did not allow them to determine the age of the formation.

4. Material and methods

A detailed geological mapping (Fig. 2) was performed in order to study stratigraphical and geometrical relationships between facies and formations. Sedimentological sections were logged by measuring the thickness of each bed and depositional environments were deduced by indexing lithologies, sedimentary

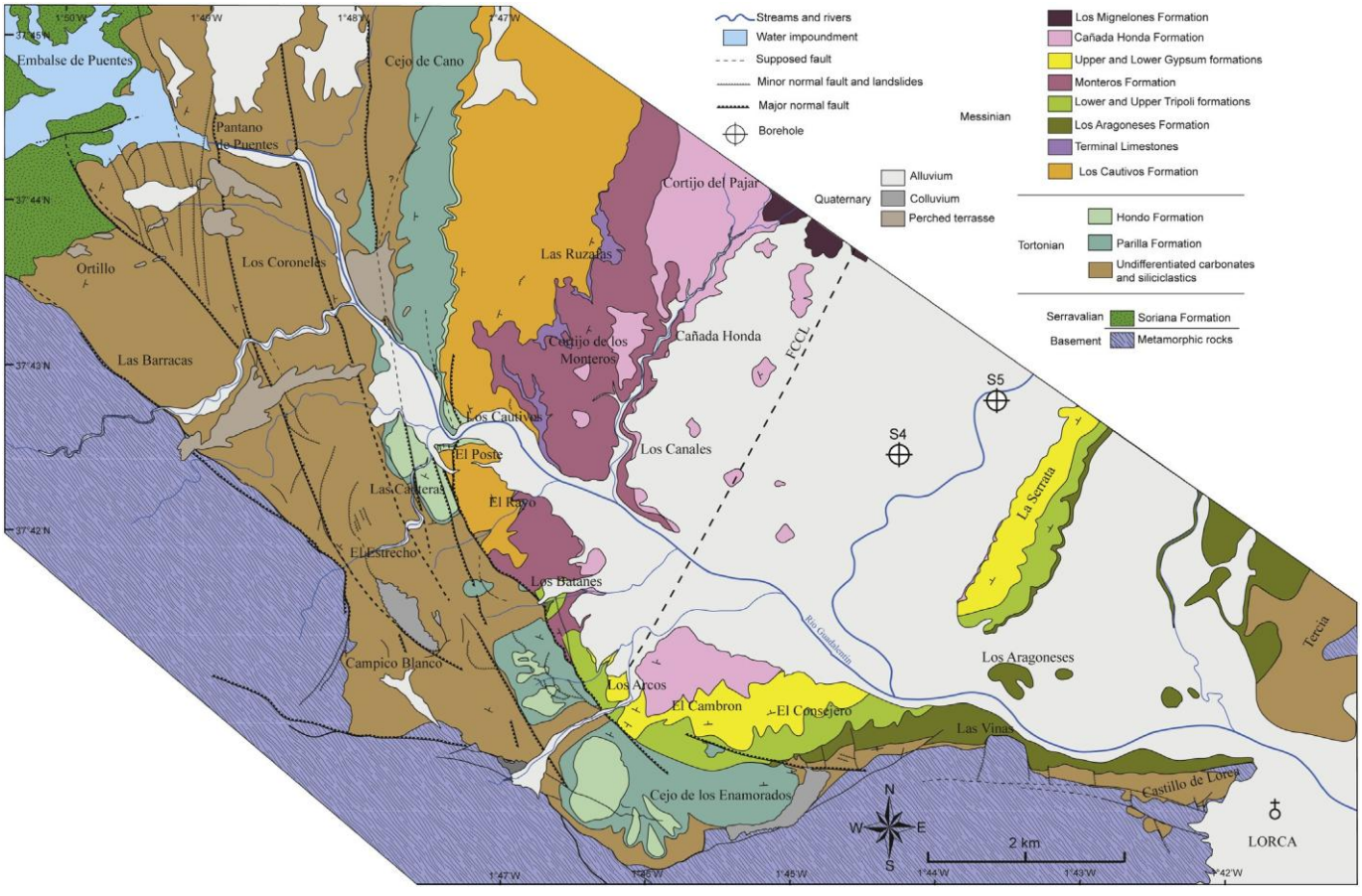

Fig. 2. Geological map of the study area (see location in Fig. 1).

structures, and the palaeontological content of deposits. The nature of surfaces (erosional, subaerial exposure, etc) was also studied in detail and indexed. Vertical facies successions and geometries at the outcrop scale were interpreted in terms of progradation, aggradation or backstepping of depositional environments reflecting the interplay between accommodation and sedimentary flux (Emery and Myers, 1996; Posamentier and Allen, 1999). Marl samples were decarbonated and sieved to determine their micropalaeontological content. Quantitative analysis of calcareous nannofossils was performed on 10 samples in the fraction of 2–30 μm, separated by decantation method using 7% solution of H_2O_2. Smearslides were mounted with Canada balsam and analysed with an Olympus transmitting light microscope, with 1200× magnification. Calcareous nannoplankton taxonomic identification follows PerchNielsen (1985) and Young (1998).

5. Results

5.1. Biostratigraphy and new lithostratigraphical framework

On the western margin, our study of nannofossils in the Crassostrearich marls of the upper part of the Parilla Fm (Fig. 3) revealed the occurrence of Amaurolithus primus suggesting a Latest Tortonian to Messinian age for this formation. According to field observations we propose a new lithostratigraphical scheme for the upper part of the sedimentary infill of the Lorca Basin corresponding to the studied interval (Fig. 3). The new lithostratigraphy fits with lithological units that can be mapped on the southern margin of the basin. The Los Cautivos Fm corresponds to the Upper pre-evaporitic unit of Wrobel and Michalzik (1999) and Serrata Fm of both Vennin et al. (2004) and Thrana and Talbot (2006). It can be subdivided into several siliciclastic or carbonate members (Fig. 3). Marine sandstones and conglomerates of the Lower and Upper Sandstone Members (Mbrs) are separated and topped by the Tarbellastrea-rich Lower and Upper Ruzafas Limestones. The upper part of the formation consists of the marine Los Cautivos Conglomerates Member (Mbr) and Porites-rich calcarenites of the Terminal Limestones Mbr. In the Los Cautivos area, the Terminal Limestones Mbr interfingers distally with white marls. Samples collected in these marls provided diatoms and Messinian nannofossils including Nicklithus amplificus and Amaurolithus spp. The overlying Monteros Fm is subdivided in several members corresponding from base to top to the marine conglomerates of the MC Mbr, variegated marls of the MM Mbr, and alluvial sandstone and

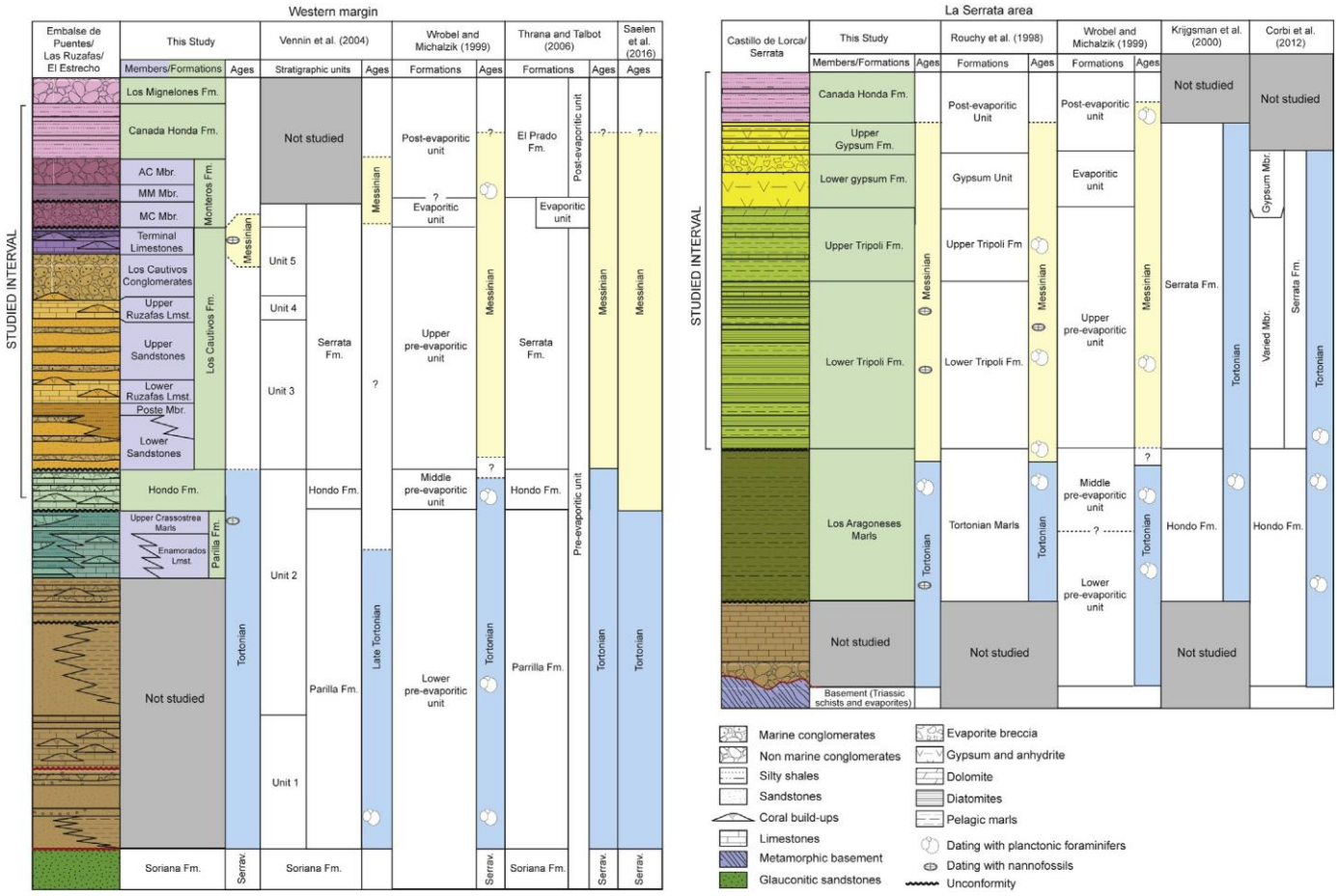

Fig. 3. Lithostratigraphy of the western margin and La Serrata area of the Lorca Basin (this study).

conglomerates of the AC Mbr. They correspond in part to the evaporitic unit of Wrobel and Michalzik (1999) and Thrana and Talbot (2006). Laminated shales and sandstone of the Canada Honda Fm and white conglomerates of Los Mignelones Fm constitute the uppermost deposits of the basin.

In the Serrata area, the Los Aragoneses Marls correspond to the Tortonian Marls of Rouchy et al. (1998) and to the Hondo Fm of Krijgsman et al. (2000). Nannofossil assemblages observed in these marls contain Amaurolithus primus that indicates a Late Tortonian to Messinian age. As explained above, the FO of G. conomiozea s.s. in the upper part of the Los Aragoneses Marls indicates the TortonianMessinian transition (C3Bn chron) and the Lower Tripoli Fm is Messinian in age. Above, three samples of the Lower Tripoli Fm yielded Reticulofenestra pseudoumbilicus and Nicklithus amplificus among others nannofossils, indicating a Messinian age (MNN1c Zone, Raffi et al., 2003) (Fig. 3). Samples also provided Amaurolithus primus and Amaurolithus delicatus whose occurrence extends from

the Tortonian/ Messinian transition to the Early Zanclean (Raffi et al., 2006). In particular, the FO of Amaurolithus delicatus was found to be coincident with the base of the Messinian at the GSSP (Global Boundary Stratotype Section and Point) for the Messinian Stage formalised at the Oued Akrech, Morocco (Hilgen et al., 2000b). The overlying Lower Gypsum Fm (Gypsum unit of Rouchy et al. (1998) and Evaporitic unit of Wrobel and Michalzik (1999)) consists of selenitic or nodular gypsum beds alternating with stromatolites (see Section 5.2 and Table 1 for a detailed description). The overlying alternation of laminated grey marls and evaporites constitutes the Upper Gypsum Fm and grades vertically to pink laminated marls devoid of evaporites of the Cañada Honda Fm. Both formations are the equivalent of the Post-evaporitic unit of Rouchy et al. (1998) and Wrobel and Michalzik (1999) and the Laminated Pelite Mbr of Garcia-Veigas et al. (2019).

5.2. Facies associations and depositional environments

Sedimentary features of facies are described in the Table 1 and in Supplementary Material (Figs. S2, S3, S4). A brief overview of the facies associations is given below.

5.2.1. Evaporite-rich facies associations

These facies associations consist of shallow hypersaline lagoon, sebkha, and muddy brackish lagoon deposits. Hypersaline lagoon deposits are characterised by an alternation of fine-grained laminated mudstones, planar stromatolites, selenitic gypsum, green marls, and sandstones (El facies, Table 1, Fig. S2A, B, Supplementary Material). Sebkha facies consist of carbonate beds or yellow sandstones locally enriched in enterolithic or chicken wire anhydrite nodules replaced by gypsum, lenticular gypsum crystals locally dissolved and forming a moldic porosity, dissolved pagoda-like halite crystals and desiccation

Table 1

Facies associations	Lithology	Geometries	Sedimentary structures and diagenetic features	Biogenic structures	Paleontological content	Interpretations
Evaporite facies	Selenite gypsum				_____	
Hypsesaline shallow lagoon: El		Lateral continuity over several hundreds of meters	Selenite gypsum locally transformed in anhydrite nodules			Subaqueous hypersaline lagoon (Warren, 2006)
	Dolomite, limestones, anhydrite	Lateral continuity over several tens of meters	Cones of anhydrite (gypsum transformation) intercalated in stromatolites, lack of dessiccation cracks	Planar stromatolites	_____	Marginal hypersaline lagoon (lower intertidal) (Alsharhan and Kendall, 2003; Warren, 2006; Bourillot et al., 2009, 2010)
Sebkha: Es	Fine to medium grained sandstones, anhydrite, gypsum, and halite	Lateral continuity over several tens of meters	Chicken wire and enterolitic nodules of anhydrite locally replaced by gypsum, dissolution vugs of lenticular gypsum crystals and of pagoda-like halite crystals, dessiccation cracks	_____	_____	Evaporitic flat (Sebkha) (Warren, 2006; Court et al., 2017)
Brackish lagoon: Eb	Grey to green mudstones, silty limestones, rare grass-like, selenite, lenticular or nodular gysum	Lateral continuity over several tens of meters	_____	_____	Ostracods, brackish foraminifera, abundant reworked Cretaceous to Paleogene foraminifera. Scarce gastropods in limestone beds	Subaqueous brackish lagoon with sporadic hypersaline conditions during phases of lowering of the water level (Rouchy and Caruso, 2006)
Siliciclastic facies		Concave up basal erosional surface		_____	_____	
Braided stream: Sb	Coarse grained sandstones and clast supported conglomerates		Trough crossbedding, internal erosional surfaces, pebble imbrications			High energy fluvial stream, cut and fill dynamic (Gh, Gt facies of Miall, 2006)
Lacustrine mudstones: Sl	Carbonated and silty mudstones	Lateral continuity over several hundreds of meters	Alternations of cm-thick carbonate and silts layers, dessiccation cracks. dm-thick gradded sandstone beds with a vertical normal grading and crude horizontal laminations	Vertical burrows	Ostracods, brackish foraminifera, abundant reworked Cretaceous to Paleogene foraminifera	Lacustrine varves with oxygenated bottom conditions and with subaerial exposure periods and flood-related deposits (Anderson and Dean, 1988; Chun and Chough, 1995; Horton and Schmitt, 1996; Buatois and Mangano, 2004)
Alluvial fan: Sa	Unsorted matrix supported conglomerates	Non-channelized and lateral continuity over several tens of meters	Slightly erosional basal surface	_____	_____	Aerial debris flows (proximal to distal alluvial fan) (Gmm facies of Miall, 2006)

	Middle to coarse grained sandstones, conglomerates	Sheet like geometry, lateral continuity over several tens or hundreds of meters, lateral transition to braided channels	Planar horizontal laminations with disseminated pebbles	_____	_____	Sheet-flood deposits (Middle to distal alluvial fan) (Fernandez et al., 1993; Kelly and Olsen, 1993; Ridgway and Decelles, 1993; Horton and Schmitt, 1996; Hampton and Horton, 2007)
	Red or variegated silts, mudstones, and carbonates	_____	Pedogenetic carbonate nodules (paleosoils stage IV to V of Retallack, 1988; Mack et al., 1993)	Root traces	Plant remains	Alluvial plain with paleosoils (Fl and P facies of Miall, 2006; FA2 facies of Hampton and Horton, 2007). Changes in redox conditions (McPherson, 1980; Miall, 2006)
	Fine to middle grained sandstones	Lateral continuity over several tens of meters	Current ripples	Root traces	_____	Overbank deposits (Sr facies of Miall, 2006)
Meandering fluvial stream: Sm	Conglomerates to middle grained sandstones	Concave up basal erosional surface and lateral pinchout	Basal pebble lag, vertical grading, epsilon cross-bedding (Allen, 1963; Miall, 2006)	Scoyenia ichnofacies (Melchor et al., 2012)	_____	Meandering channels (middle to distal alluvial fan) (Stanistreet and McCarthy, 1993; Sl, Se facies of Miall, 2006)
Gilbert delta: Sg	Non marine clast supported conglomerates	Flat toped, basal erosional surface on top of forests	Basinward pebble imbrications, internal erosional surfaces	_____	_____	Fluvial topsets (Corner et al., 1990; Postma, 1990)
	Marine clast supported copnglomerates	Lateral pinch out. Transition to topsets in a landward direction and to foresets in a basinward direction	Landward pebble imbrications within horizontal pebble ribbons. m-thick prograding conglomeratic bodies	Gastrochaenolites borings	Ostrea edulis, barnacles	Beach ribbons and small conglomeratic mouth bars (Massari and Parea, 1990; Postma, 1990)

Main sedimentological features of Messinian facies associations in the Lorca Basin.

Table 1

Facies associations	Lithology	Geometries	Sedimentary structures and diagenetic features	Biogenic structures	Paleontological content	Interpretations
Facies associations	Lithology	Geometries	Sedimentary structures and diagenetic features	Biogenic structures	Paleontological content	Interpretations
	Matrix and clast supported conglomerates, middle to coarse grained sandstones	10 m-high prograding foresets with dip up to 30°, lateral pinchouts.	Inverse gradings in clast supported conglomerates, backsets and horizontal laminations in sandstones, normal vertical gradings from conglomerates to sandstones with current ripples, lateral grading	Gastrochaenolites borings, undetermined vertical burrows in sandstones,	Ostrea Edulis, barnacles, sea-urchins	Foresets with cohesive and non-cohesive debris flows, high density turbidites, backsets, inertia-dominated homopycnal flow deposits, debris fall deposits (Postma et al., 1988; Massari and Parea, 1990; Nemec, 1990; Orton and Reading, 1993; Breda et al., 2007; Ghinassi, 2007; McConnico and Bassett, 2007; Winsemann et al., 2007, 2009)
	Fine grained sandstones and mudstones	Distal continuation of foresets, dip about 5°	Crude horizontal laminations, current ripples	Undetermined vertical burrows	Undifferentiated bivlave clasts, foraminifera	Bottomsets with middle to low density turbidites (Stow and Shanmugam, 1980; Nemec, 1990; Breda et al., 2007; Backert et al., 2010)
Submarine fan delta Proximal hyperpycnite: Sf	Fine grained calcarenite, clast supported conglomerates, coarse grained sandstones	Sheet like geometry with conglomerate ribbons laterally continuous over several tens of meters alternating with fine grained carbonates. Locally concave up basal and internal erosional surfaces with Lateral pinchout. 15 m-high and 50 m-large lensoidal geometry	Inverse gradings in clast supported conglomerates, basinward imbrication of pebbles, normal gradings and current ripples in sandstones	Gastrochaenolites borings	Oysters, pectinids, undetermined bivalves	Hyperpycnites organised in sheet like bodies in the submarine part of a fan delta or filling submarine channels crosscutting the upper part of forereef slope deposits (Cf facies) (Bøe et al., 2003; Mulder et al., 2003; Zavala et al., 2006; B1 facies of Zavala et al., 2011)
Fine grained hyperpycnite: Sw	Heterolithic, medium grained sandstones, unsorted conglomerates, mudstones	Lateral continuity over several tens of meters	Horizontal laminations, hummocky cross-stratifications, wave ripples, flaser beding	_____	Pectinids	Sandy flood-related deposits, dilute unidirectional flow at upper flow regime (Mulder et al., 2003; Zavala et al., 2006; S2h and S3w facies of Zavala et al., 2011; Steel et al., 2018)
Lower shoreface sandstones: Ss	Fine grained sandstones	Several decimeter thick bedsets intercalated in pink marls	Oscillation ripples, HCS	Skolithos burrows	Reworked Cretaceous to Paleogene foraminifera	Sand reworked by waves and storms and exported in distal marls
Carbonate facies Uppermost inner platform: Cp	Conglomerates, sandy coarse calcarenite	Lateral pinch out of pebble ribbons	Landward pebble imbrications, crude horizontal laminations	Gastrochaenolites borings	Ostrea Edulis, barnacles, Clypeaster, Scarce Porites patches	Conglomeratic beach ribbons and shallow coral patchs in an inner platform impacted by important terrigenous inputs (Vennin et al., 2004; Saelen et al., 2016)
Inner platform and reef front: Ce	Coarse grained calcarenite, gravels	0,5 to 5 m-high Tarbellastrea buildups, landward transition to uppermost inner platform environments and basinward transition to forereef deposits	_____	Undetermined vertical burrows	Tarbellastrea, Porites, coralline algae, gastropodes, oysters, pectinids, echinoderms	Well oxygenated, shallow, and agitated environment at the top of the slope (Vennin et al., 2004)
Forereef: Cf	Fine grained calcarenite, conglomerates	Several tens of m-high prograding foresets	Slumps, turbidites, conglomeratic debris flows	Undetermined vertical burrows	Undifferentiated bioclasts, bentic and planktonic foraminifera	Steep slope with gravity driven deposits below the storm wave base (Nemec and Steel, 1984; Franseen and Mankiewicz, 1991; Nemec and Postma, 1993; Johnson et al., 2005)

Basinal marls: Co	Marls, dolomite, diatomite	_____	_____	_____	Planktonic foraminifera, diatoms	Deep marine environment below the storm wave base (Rouchy et al., 1998)
Deep restricted basin: Cr	Organic-rich marls, green marls, dolomite,	_____	Slumped diatomites. Horizontal laminations, gutter casts, current ripples,	_____	Phosphatized fish remains, planktonic foraminifera	Stratified basin with turbidites, high salinity periods, and oxygen

(continued on next page)

Table 1 (continued)

Facies associations	Lithology	Geometries	Sedimentary structures and diagenetic features	Biogenic structures	Paleontological content	Interpretations
	diatomite, native sulphur, coarse grained to fine grained sandstones, selenite gypsum		load casts, normal gradings, basal erosional surfaces in sandstones			depleted conditions on the sea floor favorable to bacterial sulphate reduction (Rouchy et al., 1998; Orszag-Sperber et al., 2001; Bąbel, 2007; Andreetto et al., 2019)

cracks (Es facies, Fig. S2C, D, E, Supplementary Material). The presence of gypsum indicates the rehydratation of anhydrite formed during early diagenetic growth within fine-grained dolomitic matrix and then a formation during periods of subaerial exposure (Rouchy et al., 1998; Court et al., 2017). Brackish facies are mainly represented by grey to green mudstones containing ostracods, rare marine bentic foraminfers and abundant foraminifera reworked from the Cretaceous to the Oligocene suggesting important freshwater inputs from the continent. Mudstones contain rare tens of centimetres thick beds of silty carbonates, rare stromatolites, selenite gypsum and yellow sandstones disseminated in mudstones (Eb facies).

5.2.2. Siliciclastic facies associations

Continental facies associations consist of alluvial fan, braided river, lacustrine, and meandering river deposits. Braided river deposits are characterised by non-marine clast-supported conglomerates with metre scale trough cross-bedding and pebble imbrications (Sb facies, Table 1). Alluvial fan facies (Sa facies, Fig. S2F to J, Supplementary Material) contain channelised clast supported conglomerates intercalated or grading laterally to alluvial plain facies with palaeosoils, overbank, sheetfloods, and debris flow deposits. Meandering stream facies (Sm facies) consist of point-bar deposits with a pebble lag on their basal surface, a vertical grading and large tangential inclined beds interpreted as epsilon cross-bedding (Fig. S2K, Supplementary Material). They crosscut alluvial plain deposits. The presence of gravity-driven deposits truncating meandering channels indicates the distal part of an alluvial fan (Fig. S2L, Supplementary Material). Lacustrine facies are characterised by laminated varves, desiccation cracks, and graded sandstone beds interpreted as flood-related deposits (Sl facies, Fig. S2M, N, O, Supplementary Material).

Marine deposits correspond to Gilbert deltas, submarine fandeltas, and shoreface sandtones. Gilbert delta facies association (Sg facies) already studied by Wrobel and Michalzik (1999) in the Lorca Basin, consist of topsets made of braided river conglomerates, conglomeratic beach ribbons and mouth bars, steepened sandy and conglomeratic foresets (dip up to 30°) with gravity-driven deposits, and heterolithic bottomsets (Table 1, Fig. S3A to G, Supplementary Material). Submarine fan delta deposits correspond to an alternation of fine-grained reworked calcarenites and hyperpycnites presenting a sheet-like geometry and consisting of pebbly sandstones with inverse grading and pebble imbrication (Sf facies, Table 1, Fig. S3H, I, J, Supplementary Material). They locally infill submarine channels incised into forereef slope facies and are characterised by a basal concave upward erosional surface formed in a subaqueous environment. Distal facies (Sw facies) are heterolithic and consist of thin beds of unsorted and ungraded conglomerates alternating with yellow middle to coarse-grained sandstones containing horizontal laminations, hummocky cross-stratifications (HCS), and symmetrical oscillation ripples on top covered by lenticular mudstone interbeds (Fig. S3K, Supplementary Material). Shoreface deposits (Ss facies,

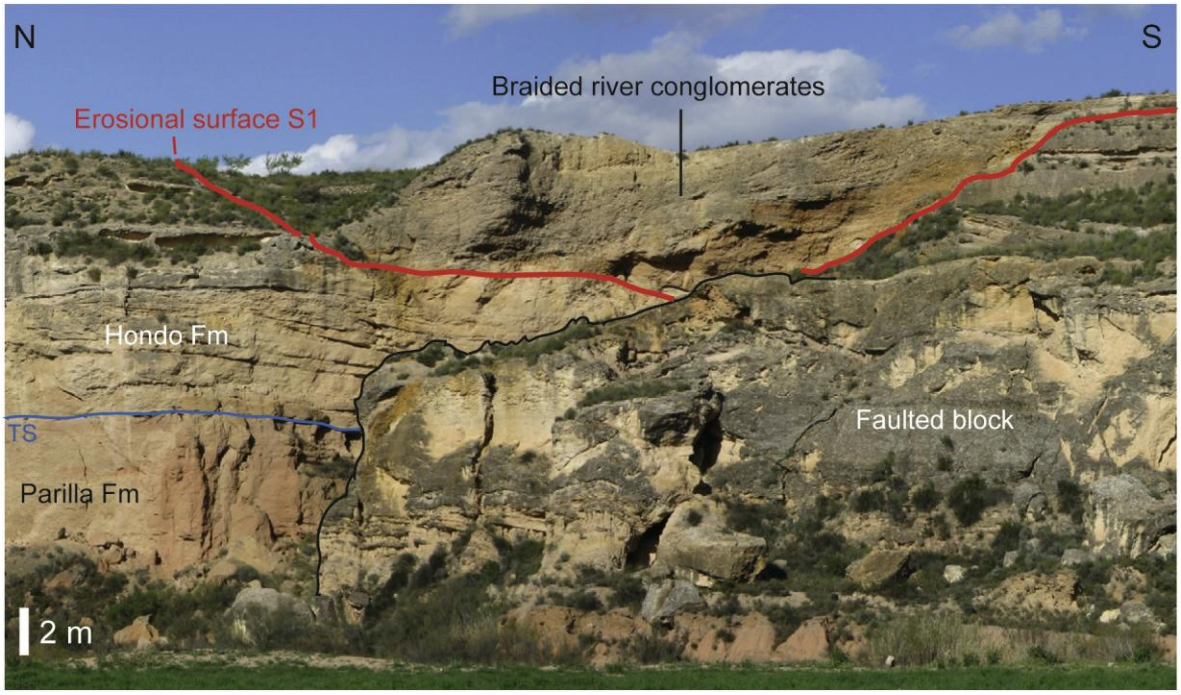

Fig. 4. Interpreted panorama of the incision at the top of the Honda Fm in the Los Cautivos area. TS = transgression surface.

Fig. 5. Panorama of the Los Cautivos area with interpreted sedimentary cycles (I to IV).

Table 1, Fig. S4A, Supplementary Material) consist of medium to fine grained sandstones with Skolithos burrows, HCS and wave ripples alternating with pink to grey mudstones.

5.2.3. Carbonate facies

Carbonate facies and reefal deposits of the Lorca Basin were described in detail by Vennin et al. (2004). The facies described here are mainly based on this work and consist of inner carbonate platform, foreslope, basinal, and deep restricted deposits. Uppermost inner platform carbonates (Cp facies, Table 1, Fig. S4A, B, Supplementary Material) are characterised by conglomeratic beach ribbons alternating with coarse-grained calcarenites and scarce Porites patches. Inner platform and reef front deposits (Ce facies, Table 1, Fig. S4D, E, Supplementary Material) consist mainly of domed and columnar Tarbellastrea with Porites in lower proportions embedded in a coarse-grained calcarenite with coral fragments, coralline algae, gastropods, oysters, pectinids and echinoderms. Forereef slope facies (Cf facies, Table 1, Fig. S4F, G, Supplementary Material) are characterised by thick foresets mainly composed of fine-grained silty calcarenites with fine-grained turbidites, slumps and conglomeratic debris flows. Basinal facies (Co facies, Table 1, Fig. S4H, Supplementary Material) are represented by yellow to grey marls rich in planktonic foraminifera. Lastly, deep restricted basin deposits (Cr facies, Table 1, Fig. S4I to N, Supplementary Material) consist of a cyclic alternation

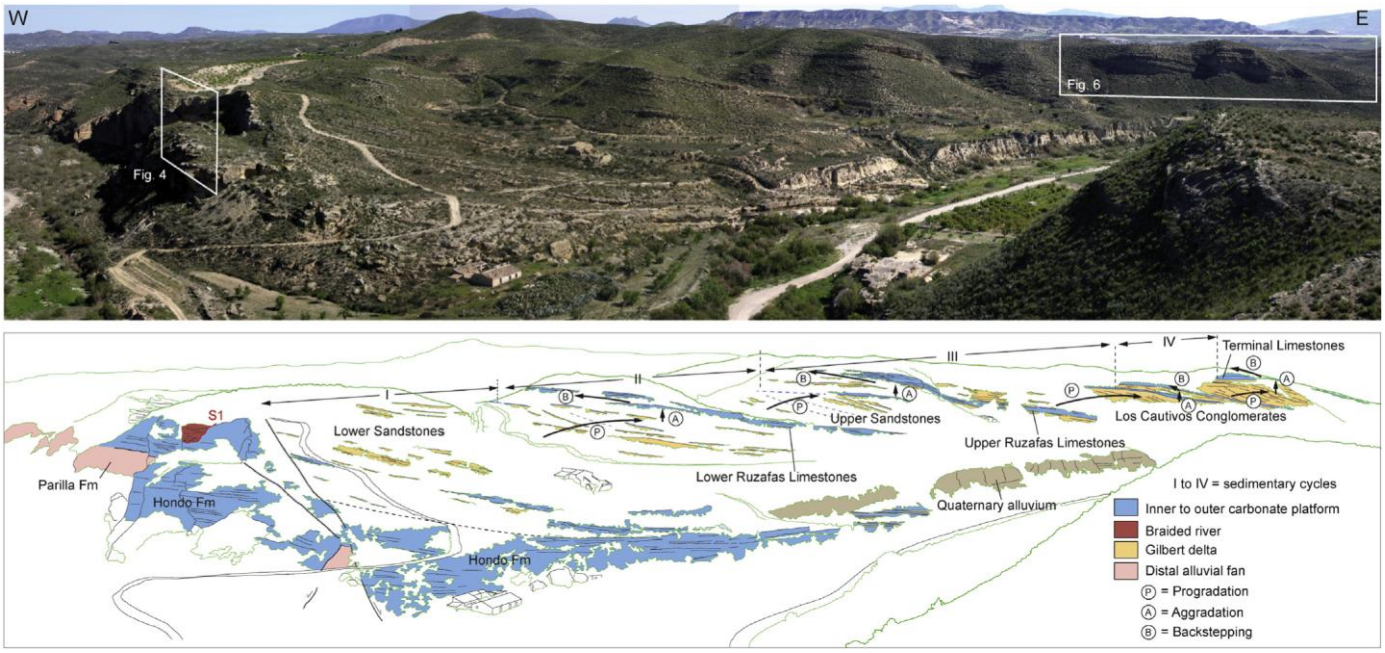

of dm-thick diatomite beds with silty green marls, limestones, dolostones, middle to coarse grained sandy turbidites, organic-rich interbeds, selenite gypsum, native sulphur, and phosphatised fish remains.

5.3. Stratigraphical architecture

5.3.1. Los Cautivos area

In the Los Cautivos area (Fig. 2), outcrops occur along the Guadalentine River. The S1 erosional surface separates the inner platform facies (Cp facies) of the Hondo Fm and the overlying Los Cautivos Fm (Fig. 4). The S1 surface is characterised by an incision of about 25 m large and 8 m deep at the top of the Hondo Fm; palaeosoils occur at its margins. The incision is filled by braided river deposits (Sb facies). Above, as already described by Wrobel and Michalzik (1999), four high frequency prograding, aggrading, and backstepping cycles labelled I to IV can be evidenced in the Los Cautivos Fm (Fig. 5). These authors described purely prograding units made of Gilbert delta sandstones and conglomerates (Sg facies) with toplap of foresets below nonaggrading fluvial topsets. These purely prograding units are covered by Gilbert delta facies with aggrading topsets where small Tarbellastrea patches appear on the surface of conglomeratic mouth bars in front of the deltaic system. Prograding and aggrading deposits correspond to the Lower Sandstones, Upper Sandstones, and Los Cautivos Conglomerates Mbrs. The marine fauna is diversified and contains barnacles, pectinids, sea-urchins, and Ostrea edulis locally organised in small buildups on the top of debris flow deposits. These prograding and aggrading units alternate with backstepping carbonates (Cp and Ce facies) characterised by a gradual landward migration of inner ramp facies and reef front facies at the expense of conglomeratic beach facies. They constitute the Lower and Upper Ruzafas Limestones Mbrs.

The prograding wedges of the two last cycles in the Los Cautivos Conglomerates (III and IV on Fig. 5) consist of 10 m high foresets (Fig. 6A) separated by carbonate units. The last prograding unit (FRP in Fig. 6A) pinches out landward on the underlying carbonate unit and its bottomsets contains dissolution features such as cavities of Tarbellastrea blocks (Fig. 6B, C). A last prograding and aggrading phase predates the onset of the Terminal Limestones Mbr. This latter is characterised by bioherms rich in Porites (Fig. 6D, E) and onlaps the top of the Los Cautivos Conglomerates (Fig. 6A). Basinward they grade laterally into fine-grained calcarenites interfingered with offshore marls containing diatoms (Co facies) and dated to the Messinian in this study (Fig. 6A). The Terminal Limestones and the upper part of the Los Cautivos Conglomerates are truncated by the erosional surface S3 that is sharply overlain by red alluvial fan deposits (Sa facies) of the Monteros Fm.

5.3.2. Cortijo de los Monteros

Between Los Cautivos and Las Ruzafas (Fig. 2) several ravines allowed us to observe the geometry of the erosional surface at the top of the Terminal Limestones. Limestones are organised in several tens of m high prograding foresets with a dip of about 20° (Fig. 7A), made of fine-grained, laminated, and locally slumped calcarenites (Cf facies) of reefal foreslope environment. They show a gradual enrichment in dm to several m thick beds of conglomeratic debris flows. Locally, submarine channels are filled by marine conglomerates with internal erosional surfaces and flood-related deposits (Sc facies). They constitute

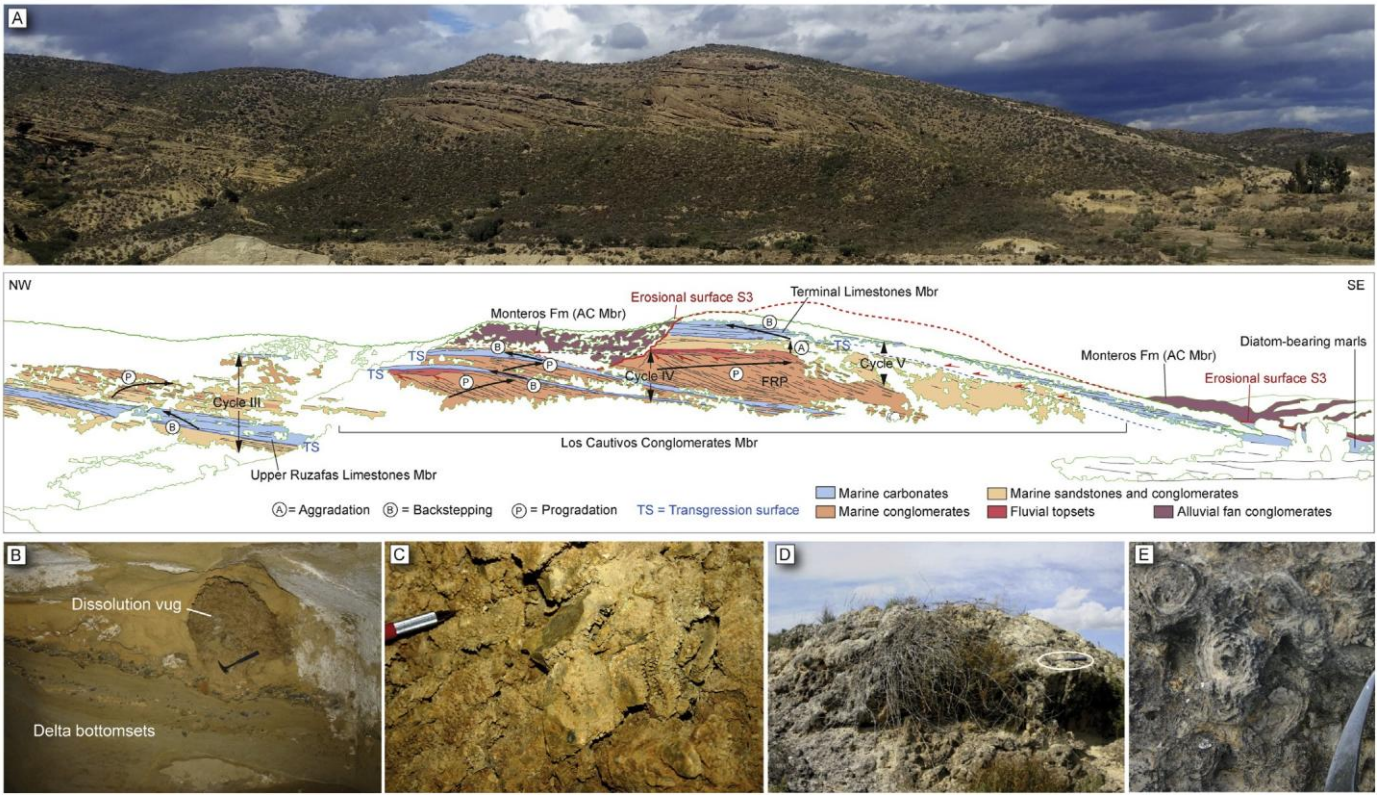

Fig. 6. Main geometries and sedimentological features of the Los Cautivos Conglomerates and Terminal Limestones in the Los Cautivos area. A) Interpreted panorama of sedimentary geometries in the Los Cautivos Conglomerates showing a gradual decrease in accommodation space and the final FRP formed in a context of forced regression. Note the final onlap of the Terminal Limestones and the overlying incision surface S3 covered by conglomerates of the Monteros Fm; B) Dissolution vug in bottomsets of the Los Cautivos Conglomerates;
C) Close-up view of the dissolution vug showing moulds of Tarbellastrea corals; D) Domed geometry of a coral buildup in the Terminal Limestones (circled hammer for scale);
E) Porites corals constituting the main builders of the Terminal Limestones.

the MC Mbr preserved in depressions above a first erosional surface (S2) at the top of the Terminal Limestones Mbr and truncated below a second erosional surface (S3) at the base of the AC Mbr (Fig. 7B). The S3 surface is characterised by several tens of m wide and about 5 m deep incisions filled by alluvial fan deposits (Sa facies) of the AC Mbr (Fig. 7C). The S3 surface lowers basinward in the progradation direction of the Terminal Limestones (Fig. 7A). Indications of subaerial exposure exist below the S3 surface and consist of abundant traces of dichotomised roots going down from the incision surface into the Terminal Limestones (Fig. 7D). Conglomerates of the AC Mbr onlap landward on the incision surface (Fig. 7E).

5.3.3. Las Ruzafas and Cañada Honda

In the Las Ruzafas area (Fig. 2) the Terminal Limestones Mbr consists of fine-grained and slumped calcarenites of foreslope environment (Cf facies, Table 1) (Fig. 8). They grade distally southeastward to offshore grey marls with diatoms and alternations of fine-grained sandy or calcarenite turbidites (Co facies). They are topped by an erosional surface (S2) covered by submarine fan delta deposits (Sf facies) of the MC Mbr (Fig. 8A). Several m large olistoliths composed of fine-grained calcarenite are embedded in the MC Mbr (Fig. 8B). Locally, the marine deposits of the MC Mbr are covered by non-marine conglomerates, which were probably deposited in a braided river system (Sb facies) over an erosional surface (S3) (Fig. 8C). Low angle sliding surfaces locally affect the distal grey marls, the Terminal Limestones, and the MC Mbr (Fig. 8D). Theses surfaces are systematically sealed by the basal fluvial conglomerates of the MM Mbr (Fig. 8D). Locally, the MC Mbr is either overlain by brackish marls (Eb facies) of the MM. Mbr or by alluvial fan deposits of the AC Mbr (Fig. 8C, E). The MC Mbr is tilted to the east with a dip of about 10° to 15° while the overlying marls show a dip of 5° in the same direction (Fig. 8C). The contact between the MM Mbr and the overlying alluvial fan deposits of the AC Mbr is sharp and slightly erosional (Fig. 8E).

The upper part of the Messinian deposits can be observed at Cañada Honda and Cortijo del Pajar (Fig. 2). In this area the Ac Mbr is characterised by intermediate alluvial fan facies and is covered by the Cañada Honda Fm consisting of an alternation of intermediate and distal alluvial fan deposits with meandering channels (Sa and Sm facies). The upper part of the Cañada Honda Fm consists of distal alluvial fan deposits.

5.3.4. Southern margin

The southern margin of the basin is crosscut by a N140° trending normal fault (Fig. 2). The hanging wall consists of Messinian deposits in faulted contact against Tortonian carbonates of the footwall. Several valleys perpendicular to the basin margin allowed us to log and correlate ten sections between El Rayo and El Consejero (Fig. 9). Along the Barranco El Rayo, distal facies of the Terminal Limestones consist of marls containing fine-grained calcarenite beds and diatoms (Co facies). They are truncated by an erosional surface (S2) deepening basinward (Fig. 10A). The surface is onlapped by alluvial fan conglomerates (Sa facies) of the Monteros Fm (MC Mbr). Between El Rayo and Los Batanes, alluvial fan facies directly overlying the Terminal Limestones are enriched in sandstones and channelised conglomerates become scarce and are replaced by conglomerate ribbons or sheets interpreted as overbank and sheetflood deposits of

intermediate alluvial fan environment (Fig. 9). In the Los Batanes area basal conglomerates become marine and are organised in matrix-supported debris flows with reworked Tarbellastrea pebbles (Fig. 10B) and coarse-grained deposits of submarine fan delta environment like those observed in the MC Mbr in the Las Ruzafas area (Sf facies). They cover grey offshore marls through a sharp erosional contact corresponding to the S2 surface

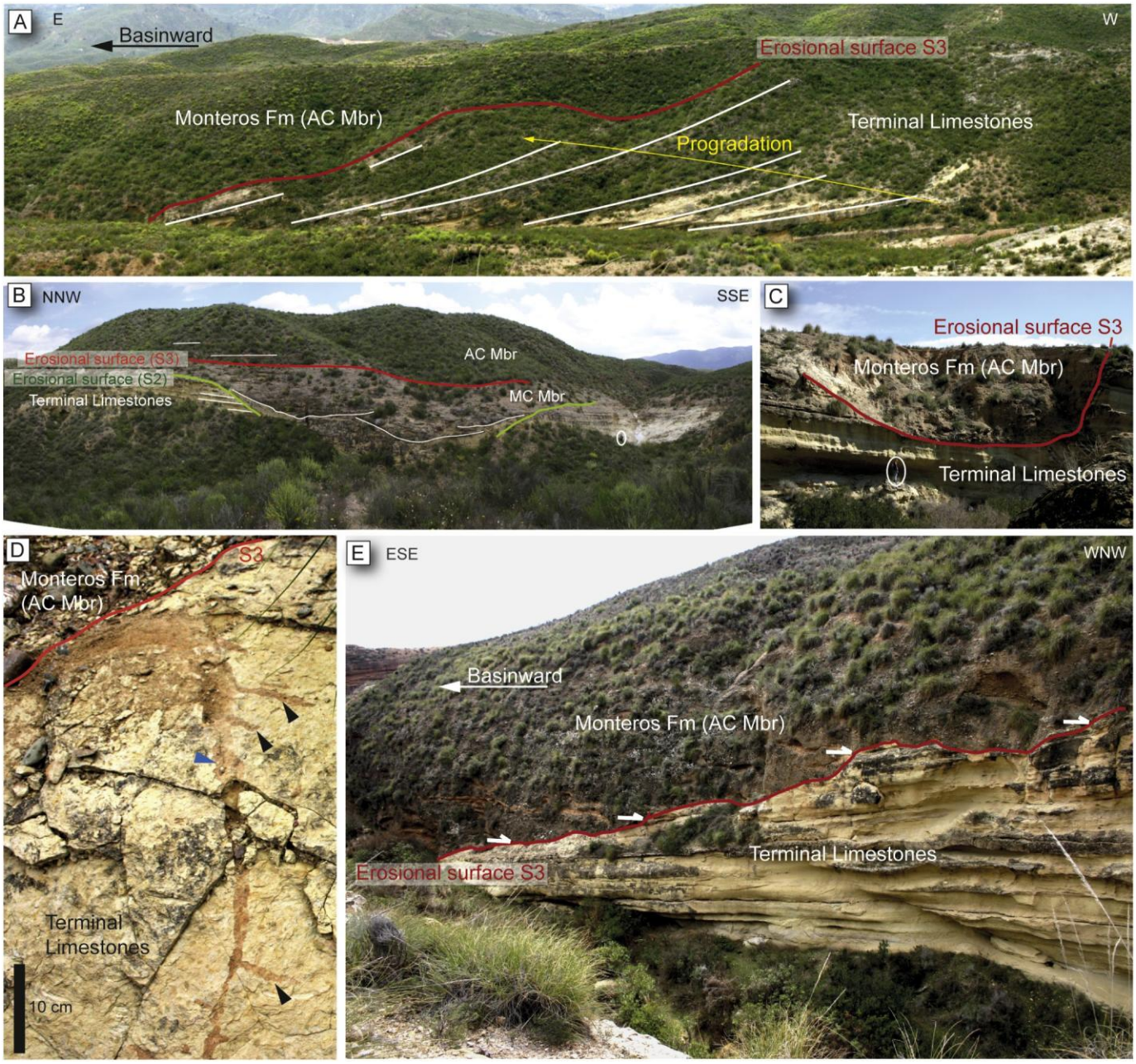

Fig. 7. Stratigraphical architecture of the Cortijo de los Monteros area. A) Prograding foresets in foreslope deposits of the Terminal Limestones incised by a major erosional surface (S3); B) Subaqueous canyon characterised by an erosional basal surface (S2, green line) incising in carbonate platform slope deposits. Note the internal erosional surfaces (white lines) with a concave-up geometry. The upper surface corresponds to a surface of subaerial exposure covered by alluvial conglomerates of the AC Mbr. Circled geologist for scale; C) Incised valley filled by alluvial conglomerate of the AC Mbr. Circled geologist for scale; D) Root trace (blue arrow) below the incision surface S3 at the base of AC Mbr. Note the dichotomisation of rootlets (black arrows); E) Onlap geometry of the AC Mbr on the incision surface S3. (For interpretation of the references to colour in this figure legend, the reader is referred to the web version of this article.)

(Fig. 10C). To the southeast, in El Cambron and El Consejero, The MC Mbr is characterised by yellow sandstones consisting of distal hyperpycnites (Sw facies) covering the Tripoli Fm through the sharp S2 surface (Fig. 10D). In this area the contact between the Los Aragoneses Marls and the overlying Tripoli Fm is sharp and locally erosional (S1 surface) (Figs. 9, 10E). Normal faults cutting through Limestones of the Parilla Fm and diatomites were observed. The surface of the Cejo de los Enamorados is notched by valleys perpendicular to the basin margin (Fig. 10F). This surface (S1 surface) is unconformable with respect to the bedding of the Tortonian limestones (Fig. 10G). The Hondo Fm pinches out eastward on top of the Parilla Fm and is absent in the area of the Cejo de los Enamorados. Diatomites of the Tripoli Fm, which were deposited in a deep restricted basin (Cr facies), onlap the S1 surface and fill incisions at the top of the Cejo de los Enamorados (Fig. 10G).

Between Los Arcos and El Consejero an evaporitic unit (Lower Gypsum Fm) rich in stromatolites, laminated mudstones, and sandstones covers the yellow sandstones of the MC Mbr (Fig. 11A). In the lower part of the unit, gypsum is mainly characterised by sebkha facies (Es facies). Subaqueous salina facies become more abundant in the upper part. The thickness of the Lower Gypsum Fm increases gradually in the El Consejero direction (Fig. 9). The Lower Gypsum Fm is capped by a palaeosoil (S3 surface) containing red mudstones alternating with sandy carbonates of sebkha environment presenting dissolution vugs of lenticular gypsum crystals (Es facies) (Fig. 11B). The uppermost bed shows evidence of

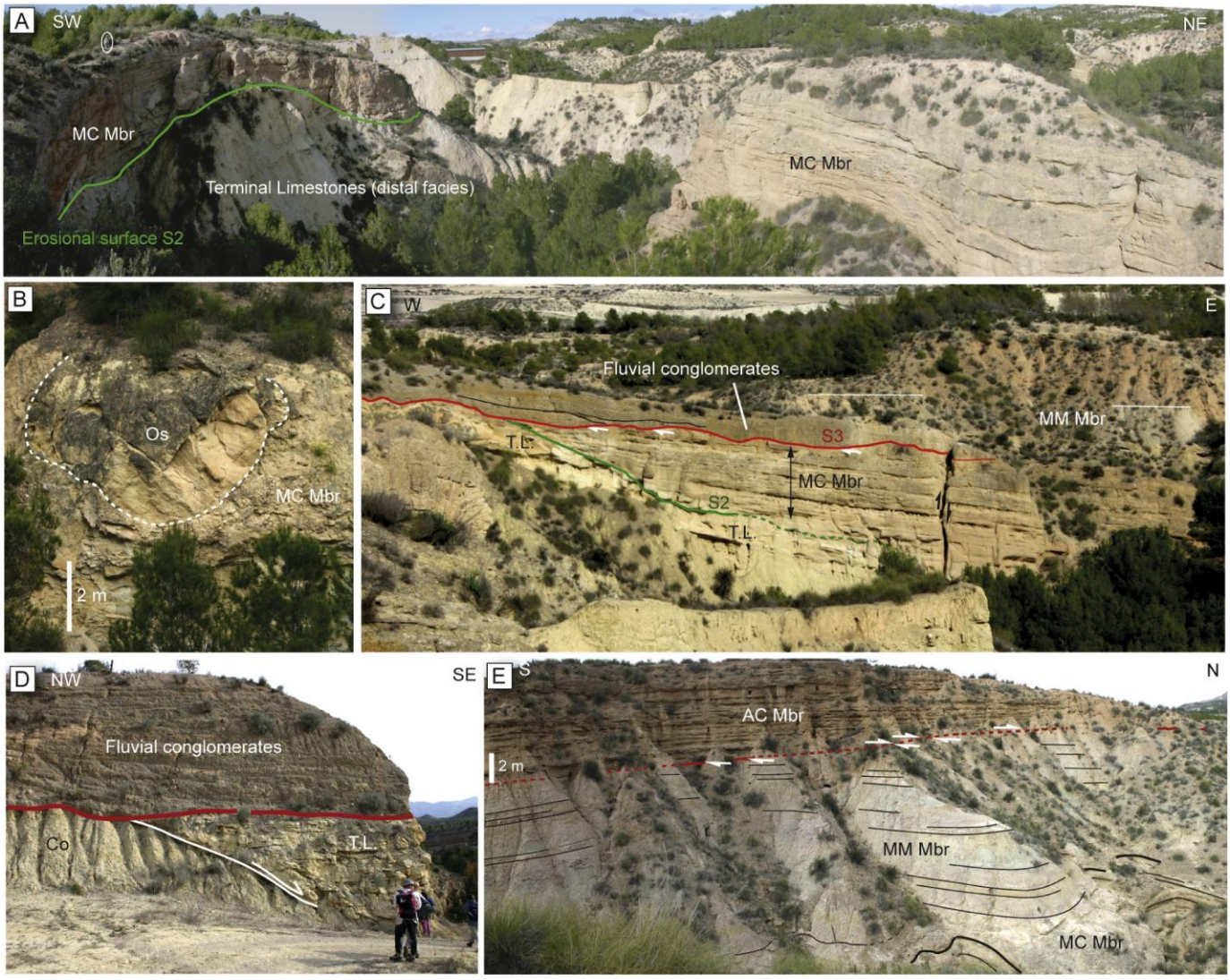

Fig. 8. Sedimentary features in the Las Ruzafas area. A) Incision surface S2 between distal facies of the Terminal Limestones and coarse grained turbidites of the MC Mbr. Circled geologist for scale; B) Calcarenite olistolith (Os) provided by the erosion of the Terminal Limestones and incorporated in marine conglomerates of the MC Mbr; C) Global view of the stratigraphical relationships between the Terminal Limestones, the MC Mbr, and the MM Mbr. The incision surface (S2) between the Terminal Limestones (TL) and the MC Mbr is sealed by braided river conglomerates above the S3 surface. Note the difference in dip between the MC Mbr and the brackish marls of the MM Mbr; D) Sliding surface between offshore marls (Co) and the Terminal Limestones (T.L.) sealed by braided river conglomerates; E) Slight erosional contact between brackish variegated marls of the MM Mbr and alluvial fan deposits of the AC
Mbr. Note the difference in dip between the MC and MM Mbrs.

subaerial exposure such as vertical cm-sized root traces still containing organic remains (Fig. 11C). Southeast of Los Arcos, beds can be intensively folded and folds are generally overturned in a basinward direction. Rouchy et al. (1998) noted that fold axes present a quite constant direction around N210° suggesting that the deformation was due to massive sliding of evaporites during a subsequent tilting of the basin. Because of the poor quality of outcrops and the intensive deformation of evaporites this surface was not mapped at the top of the Lower Gypsum Fm in this area. In contrast, northwest of Los Arcos the Lower Gypsum Fm is incised (S3 surface) and covered by massive unsorted debris flow deposits (Fig. 11D). These deposits pinch out toward Los Batanes and they can be differentiated from tabular Quaternary alluviums since they are tilted to the northeast and locally covered by brackish variegated marls of the Upper Gypsum Fm. In Los Arcos, the surface of subaerial exposure is covered by brackish lake deposits with evaporite alternations (Eb facies) of the Upper Gypsum Fm (Fig. 9). In the upper part of the formation, gastropods and sebkha deposits are locally present in limestones as well as desiccation cracks at the top of some mudstone beds.

In the Los Batanes area the Lower Gypsum Fm is absent and marls of the Upper Gypsum Fm containing clusters of primary palmate gypsum cover marine conglomerates of the MC Mbr through a sharp erosional contact (S3 surface) (Fig. 11E). This surface is onlapped by the Upper Gypsum Fm. Evaporite marls are covered by pink marls with wavedominated sandstones of shoreface environment (Ss facies) in the lower part of the Cañada Honda Fm (Fig. 11F). Overlying deposits are enriched in sandstones and conglomerates containing small oyster shells and undetermined bivalves (Fig. 11G). In the Los Arcos area the vertical

transition from the Upper Gypsum to the Cañada Honda Fm is gradual and is characterised by the disappearance of gypsum beds. Sandy flood-related deposits and then crossbedded sandy fluvial channels appear in the upper part of the section (Figs. 9, 11H). The Upper Gypsum Fm disappears toward El Rayo. In this direction, wavedominated deposits grade laterally to distal and then to intermediate alluvial fan deposits, which onlap the top of the MC Mbr (Fig. 11I).

5.3.5. La Serrata

The Serrata outcrop consists of a NE-SW oriented ridge (Fig. 2). It exposes the vertical transition from the Aragoneses Marls Fm, to the Messinian Lower and

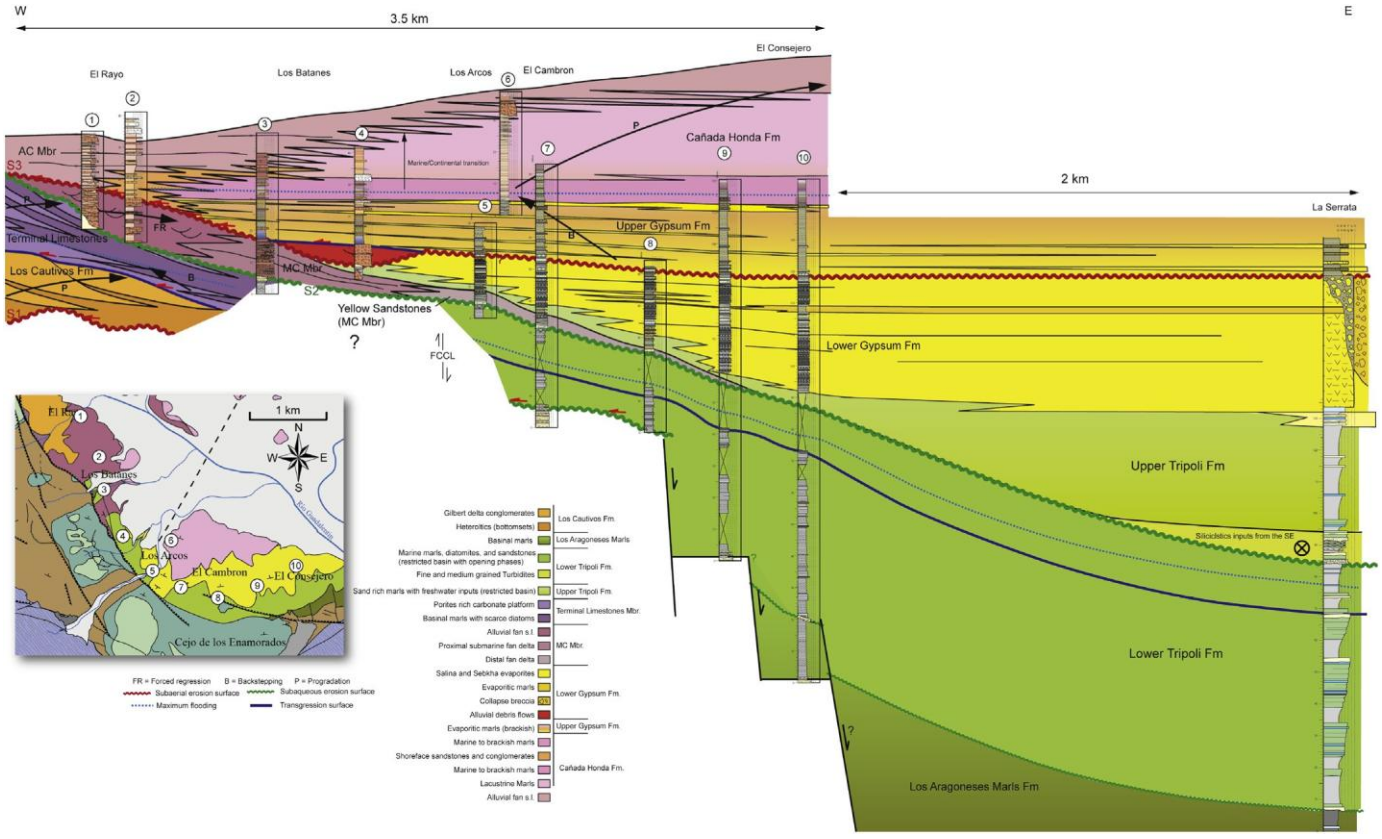

Fig. 9. Stratigraphical architecture of the southern margin of the Lorca Basin.

Upper Tripoli Fm, and the Lower Gypsum Fm (Fig. 12A). Several sections were logged in detail by Rouchy et al. (1998) and their observations are introduced in this study. The Aragoneses Marls Fm is characterised by basinal grey marls with scarce nodular dolostone beds (Co facies). Part of the foraminifera assemblages observed in these marls was reworked from the Cretaceous to the Middle Miocene (Rouchy et al., 1998). The transition to the Lower Tripoli Fm is sharp (S1 surface) (Fig. 12B) and is characterised by a stratigraphical gap of several hundred or thousand years (Rouchy et al., 1998). The deposits of the Lower Tripoli Fm are organised in five sequences starting with offshore silty marls (Co facies) and grading vertically to diatomites (Cr facies) with some limestone beds (Figs. 12C, 13). A gradual increase in the thickness of diatomite beds and an enrichment in sandstones characterise the Lower Tripoli Fm (Fig. 12B). Evaporite-derived minerals such as native sulphur are present in diatomite beds. Slumped diatomites showing a westward displacement are sometimes present on top of sequences. The amount of sandy turbidites and non-cohesive grain flows increases in the upper 10 m of the Lower Tripoli Fm. Gutter casts on the basal surface of grain flows indicate a N310° direction of transport. In contrast, the Upper Tripoli Fm is mainly made of silty marls (Fig. 13). Thin carbonate beds are present in its lower part while an increase in dolomite, sandstone, and conglomerate beds occurs in the upper part (Fig. 13). Diatomites beds and evaporitederived minerals are absent in the Upper Tripoli Fm.

The contact between the Upper Tripoli Fm and the Lower Gypsum Fm is sharp (Fig. 12A). Conglomerates were described by Rouchy et al. (1998) just below the contact. The deposits of the Lower Gypsum Fm consist of an alternation of evaporites, sandstones and stromatolites of sebkha and shallow salina environment (Es and El facies). Halite pseudomorphs and sebkha facies have been observed in the Lower Gypsum Fm.

6. Discussion

6.1. Basin wide correlations and palaeogeography

The ages that we have obtained indicate that the Tortonian carbonates of the Parilla and Hondo Fms and the Los Aragoneses Marls Fm are partly coeval as envisaged by Krijgsman et al. (2000) (Fig. 3). In the western part of the basin, carbonate facies containing a diversified benthic fauna with Porites and Tarbellastrea buildups of the Hondo Fm are typical of a shallow marine tropical platform (Brachert et al., 2001; Braga et al., 2006; Martin et al., 2010). In the eastern part of the basin the Tortonian Los Aragoneses Marls were also deposited in a normal marine environment (Rouchy et al., 1998). The abundance of foraminifera reworked from the Cretaceous to the Middle Miocene indicates that most terrigenous inputs were provided by the erosion of the External Betics located to the west. The

palaeogeographical configuration with shallow carbonate systems on the western and southwestern margin grading on a short distance to offshore marls in the Serrata area indicates that this latter region was the area with the most pronounced subsidence at the end of the Tortonian (Fig. 14A).

A first base-level drop was recorded by the S1 surface (Fig. 14B). In the area of the Cejo de Los Enamorados (Fig. 2), this base-level drop and a probable subaerial exposure of the southeastern margin prior to the deposition of diatomites are characterised by basinward oriented incisions (S1 surface) onlapped by the Lower Tripoli Fm on top of the Parilla Fm. This event is also suggested by the sharp and erosional contact between offshore marls of the Los Aragoneses Fm and the Lower Tripoli Fm. According to Rouchy et al. (1998), a stratigraphical gap and a drop in relative sea-level of at least 50 m occurred between these formations. However a gravitational collapse of the platform margin prior to the incision cannot be excluded since i) the truncation surface is strongly oblique compared with the limestone stratification, ii) the

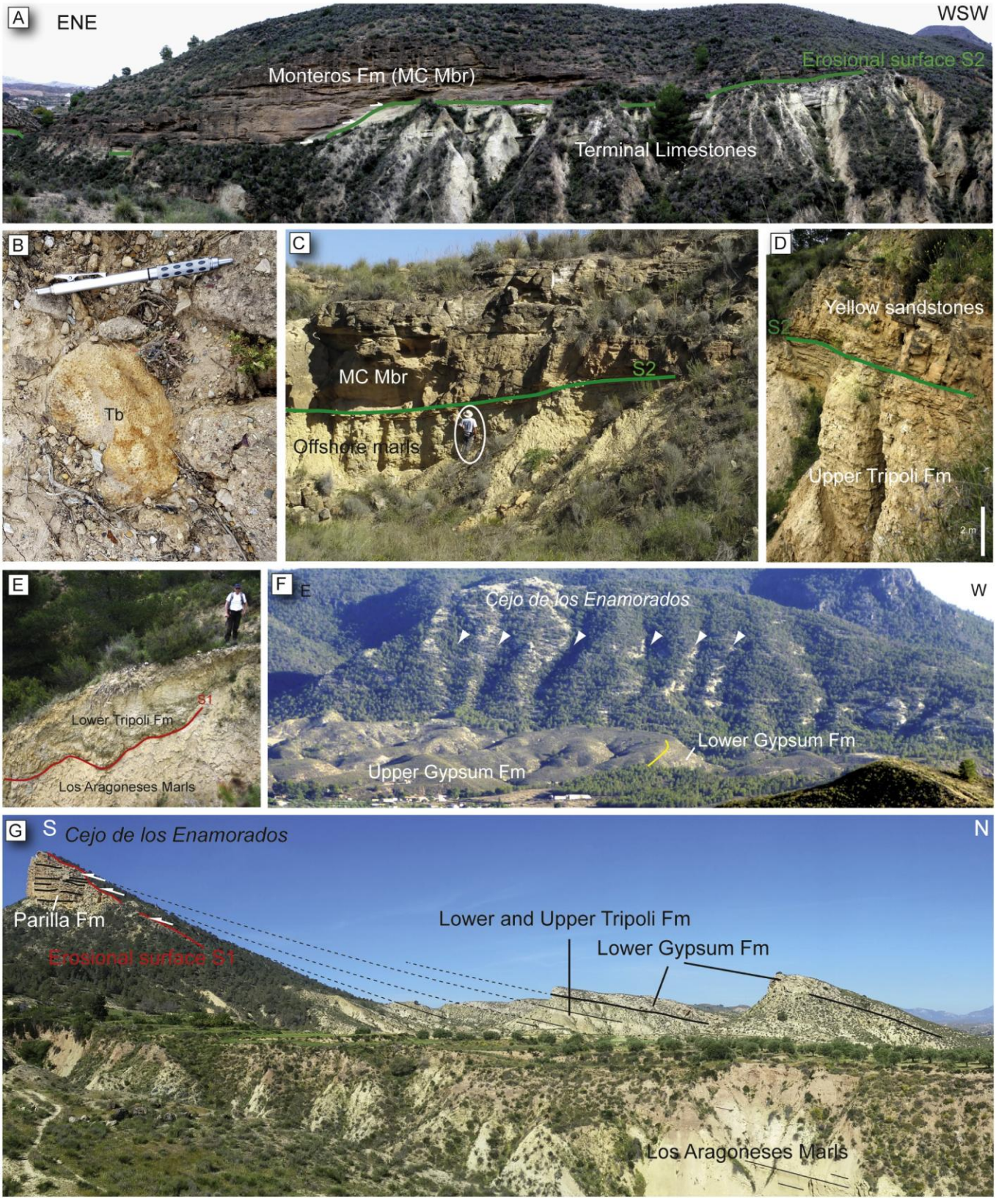

Fig. 10. Mainsedimentary features of the southern margin of the LorcaBasin (part 1). A) Incision surface S2 between distal facies of the Terminal Limestones characterised bydistaldiatombearing marls and alluvial fan deposits of the MC Mbr (Barranco El Rayo); B) Rounded Tarbellastrea pebble in the MC Mbr (Los Batanes); C) Sharp contact (S2 surface) between offshore marls and coarse-grained turbidites of the MC Mbr Circled geologist for scale (Los Batanes); D) Sharp contact (S2 surface) between the Upper Tripoli Fm and yellow shoreface sandstones in El Cambron; E) Erosional contact (S1 surface) between offshore marls of the Los Aragoneses Fm and diatomites of the Lower Tripoli Fm; F) Incised valleys (arrows) perpendicular to the basin margin on the upper surface of the Cejo de Los Enamorados formed by the Parilla Fm; G) Panorama of the southern face of the Cejo de Los Enamorados allowing to observe the strong obliquity of the erosional surface (S1 surface) with respect to the beding of the Parilla Fm and the onlap deduced by the difference in dip between the Tripoli Fm, the Lower Gypsum Fm, and the erosional surface. (For interpretation of the references to colour in this figure legend, the reader is referred to the web version of this article.)

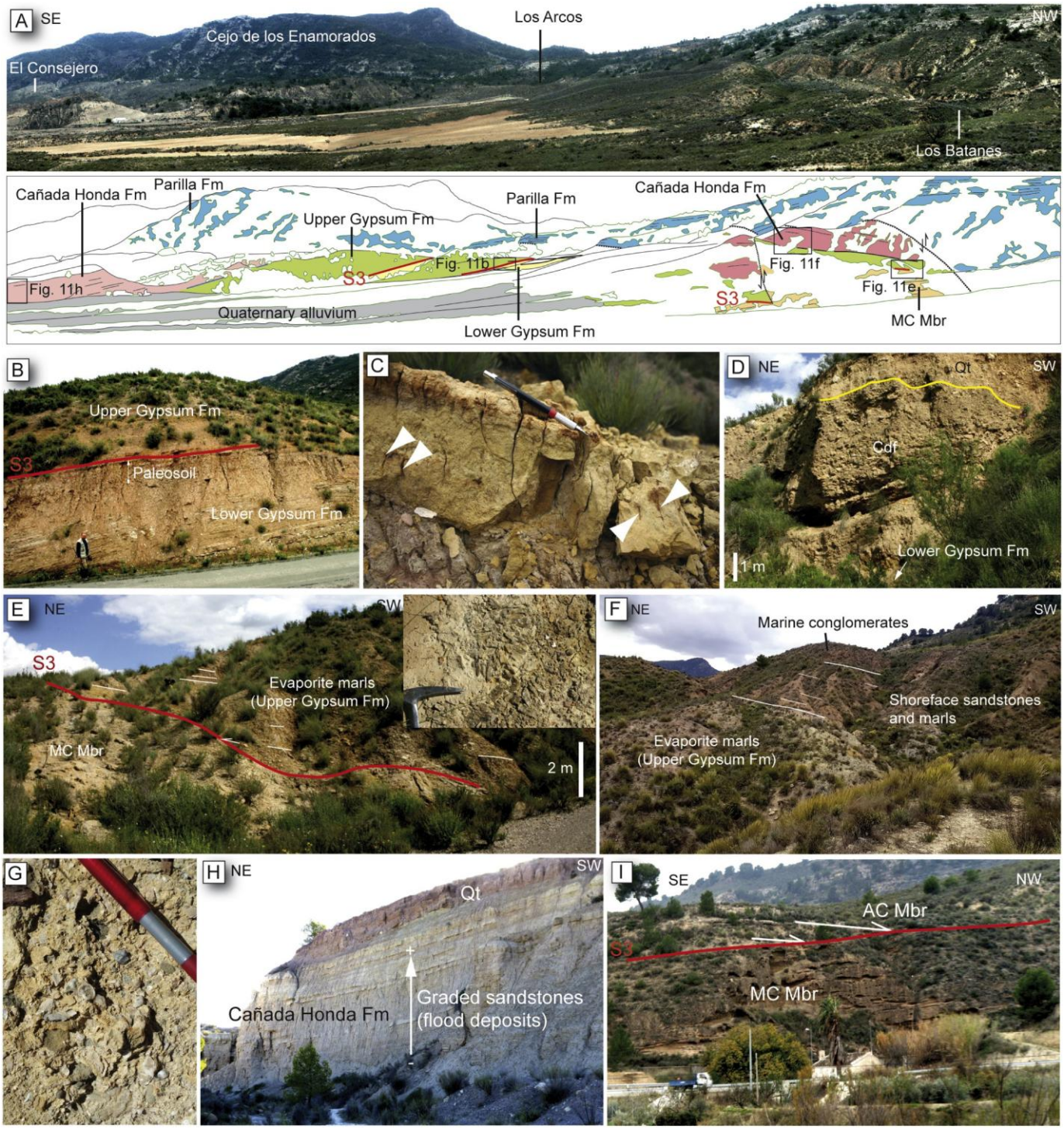

Fig. 11. Main sedimentary features of the southern margin of the Lorca Basin (part 2); A) Interpreted panorama of the southern margin between Los Batanes and Los Arcos; B) Palaeosoil at the top of the Lower Gypsum Fm in Los Arcos (see location in Fig. 10A); C) Calcrete with root traces (arrows) at the top of the palaeosoil; D) Massive continental debris flows (Cdf) intercalated between Lower and Upper Gypsum Fms between Los Batanes and Los Arcos. Deposits are tilted to the northeast while the contact with Quaternary alluvium (Qt) is quite horizontal; E) Erosional contact between the coarse-grained turbidites of the MC Mbr and evaporitic marls of the Upper Gypsum Fm. The insert shows a cluster of palmate gypsum in the evaporitic marls (see location in Fig. 10A); F) Vertical transition from evaporite marls (Upper Gypsum Fm) to marls with wave modeled sandstones and to marine conglomerates (see location in Fig. 10A); G) Abundant oysters shells in the AC Mbr in Los Batanes; H) General view of the Cañada Honda Fm in the Los Arcos area (see location in Fig. 10A). Note the vertical enrichment in sandy flood-related deposits in the upper part of the formation (Qt = Quaternary alluvium); I) Onlap of middle alluvial fan deposits of the AC Mbr on the roof
of the MC Mbr (Barranco El Rayo).

surface shows a very straight appearance in the basinal direction, iii) Rouchy et al. (1998) identified a repeated interval of about 130 m in thickness rich in large carbonate blocks in the Tortonian marls of the Serrata area that they interpreted as a collapse of the platform margin.

This first base-level drop was also recorded on the western margin of the basin where it consists of the incision at the top of the Hondo Fm in the Los Cautivos area (Fig. 14B). Here, palaeosoils preserved on channel margins and overlying braided river deposits of the Los Cautivos Fm,

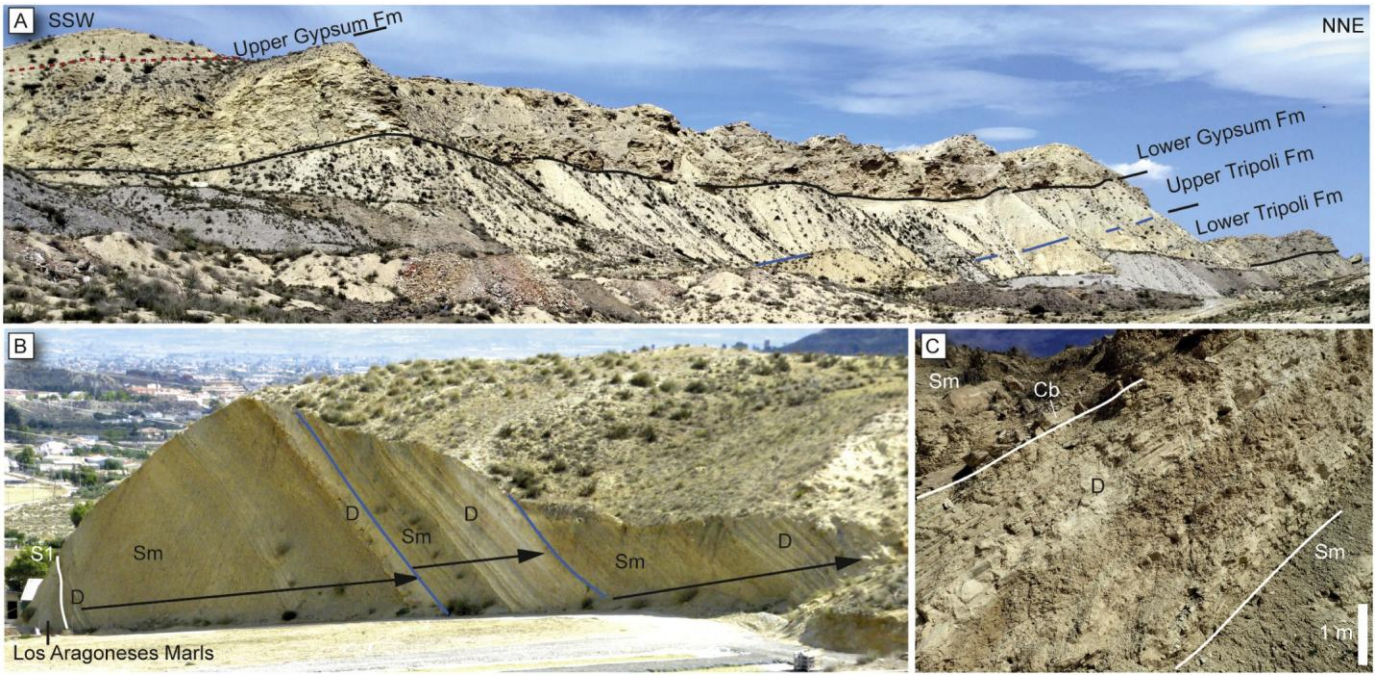

Fig. 12. Main sedimentary features in the Serrata. A) Panoramic view of the Serrata ridge; B) Stacking of restriction cycles characterised by the gradual transition between offshore silty marls (Sm) and diatomites (D) in the Lower Tripoli Fm. Cycles are separated by a flooding surface (blue line) located at the transition between diatomites and offshore marls. Note the sharp contact between Los Aragoneses marls and the Lower Tripoli Fm (S1 surface); C) Close-up view of the transition between basinal marls (Sm) and diatomite beds (D). The top of cycles are sometimes capped by slumped diatomites or limestones beds (Cb). (For interpretation of the references to colour in this figure legend, the reader is referred to the web version of this article.)

formed during a phase of creation of accommodation space. During the deposition of aggrading deltaic conglomerates and carbonate facies of the Los Cautivos Fm the occurrence of diversified eurihaline fauna suggests that normal marine conditions prevailed in the basin, at least in shallow areas. The growth of Tarbellastrea patches on mouth bar deposits during aggradation phases predated the generalised development of Tarbellastrea bioherms onlapping on deltaic sandstones and conglomerates and grading landward to inner ramp conglomeratic carbonates during the backstepping phases (Vennin et al., 2004). The proliferation of the carbonate production was favoured by a decrease in siliciclastic inputs caused by an increase in the accommodation space or only linked to a decrease in continental erosion during climatic variations. This question will be addressed in the Section 6.2. In the Los Cautivos Fm, the gradual disappearance of aggrading deposits from cycles I to IV and the reduced thickness of transgressive carbonate deposits during the high frequency cycle IV (Los Cautivos Conglomerates Mbr) (Fig. 6) indicate that the long-term accommodation space decreased gradually with time. This trend led to the formation of the last prograding wedge (FRP in Fig. 7A) pinching out landward on older carbonate deposits. This geometry is considered as an indication of forced regression during a period of relative sea-level drop (Hunt and Tucker, 1992; Plint and Nummedal, 2000; Catuneanu et al., 2009). This phase led to the erosion of underlying carbonates as evidenced by the occurrence of reworked Tarbellastrea blocks embedded in bottomset deposits.

In the Serrata area, the five cycles observed in the Lower Tripoli Fm are interpreted as cycles of opening and restriction of the basin (Benali et al., 1995; Rouchy et al., 1998; Jurkschat et al., 2000) (Fig. 13). Silty marls devoid of diatomites and evaporites correspond to periods of unrestricted basin conditions. In contrast, transitions to diatomites, organic shales, evaporite-derived minerals, and sandstone beds occurred when the basin became confined. Rouchy et al. (1998) observed sebkha facies in the northeastern part of the Serrata outcrop suggesting that during restricted periods the water-level lowered and margins were temporarily exposed. The overall increase in siliciclastic inputs at the top of the Lower Tripoli suggests an overall shallowing-upward trend. The occurrence of slumps at the top of some sequences indicates that failures of basin margins predated the reopening of depositional environments and the deposition of silty marls.

No direct observations in the field allowed us to observe the lateral transition between the Gilbert delta deposits and Terminal Limestones of the Los Cautivos Fm and the diatomites of the Lower Tripoli Fm. However, several arguments allow to support such a correlation: i) these formations overlie the incision surface S1 at the top of the Parilla and Hondo Fms at the Cejo de Los Enamorados and Los Cautivos; ii) the Messinian dating in the Tripoli Fm is in accordance with ages proposed by Rouchy et al. (1998) and Wrobel and Michalzik (1999) and only the lower part of the Serrata section is Late Tortonian. The Lower Tripoli Fm. is dated to the Messinian and a similar age was proposed by Wrobel and Michalzik (1999) and Saelen et al. (2016) for the Los Cautivos Fm; iii) five high frequency cycles of progradation-aggradation-backstepping or opening-restriction exist in the Los Cautivos and Lower Tripoli Fm, respectively (Fig. 14C). The overall progradation during the deposition of conglomerates on the western margin is also recorded by the overall increase in siliciclastics in the Lower Tripoli Fm (Fig. 14D). The proliferation of diatoms in the Lower Tripoli Fm was favoured by continental inputs providing silica and nutrient-rich waters (Playà et al., 2000; Pellegrino et al., 2018). Such conditions were certainly encountered when Gilbert delta systems formed on the western margin of the basin (Rouchy et al., 1998) (Fig. 14C, D). In the Lower Tripoli Fm, abundant foraminifera reworked from the External Betics also indicate that the majority of sediments was supplied by the western margin (Rouchy et al., 1998). Aggradation and backstepping periods that led to the development of Tarbellastrea-rich carbonates in the Los

Cautivos Fm were accompanied by a rise in relative sea-level. These events periodically led to the reentering of marine waters into the basin and the attenuation of restricted conditions in the Tripoli Fm with the deposition of offshore marls. In contrast, at the end of progradation periods, accommodation was null or negative, as indicated by purely prograding wedges or forced regressions in the Los Cautivos Fm, and favoured

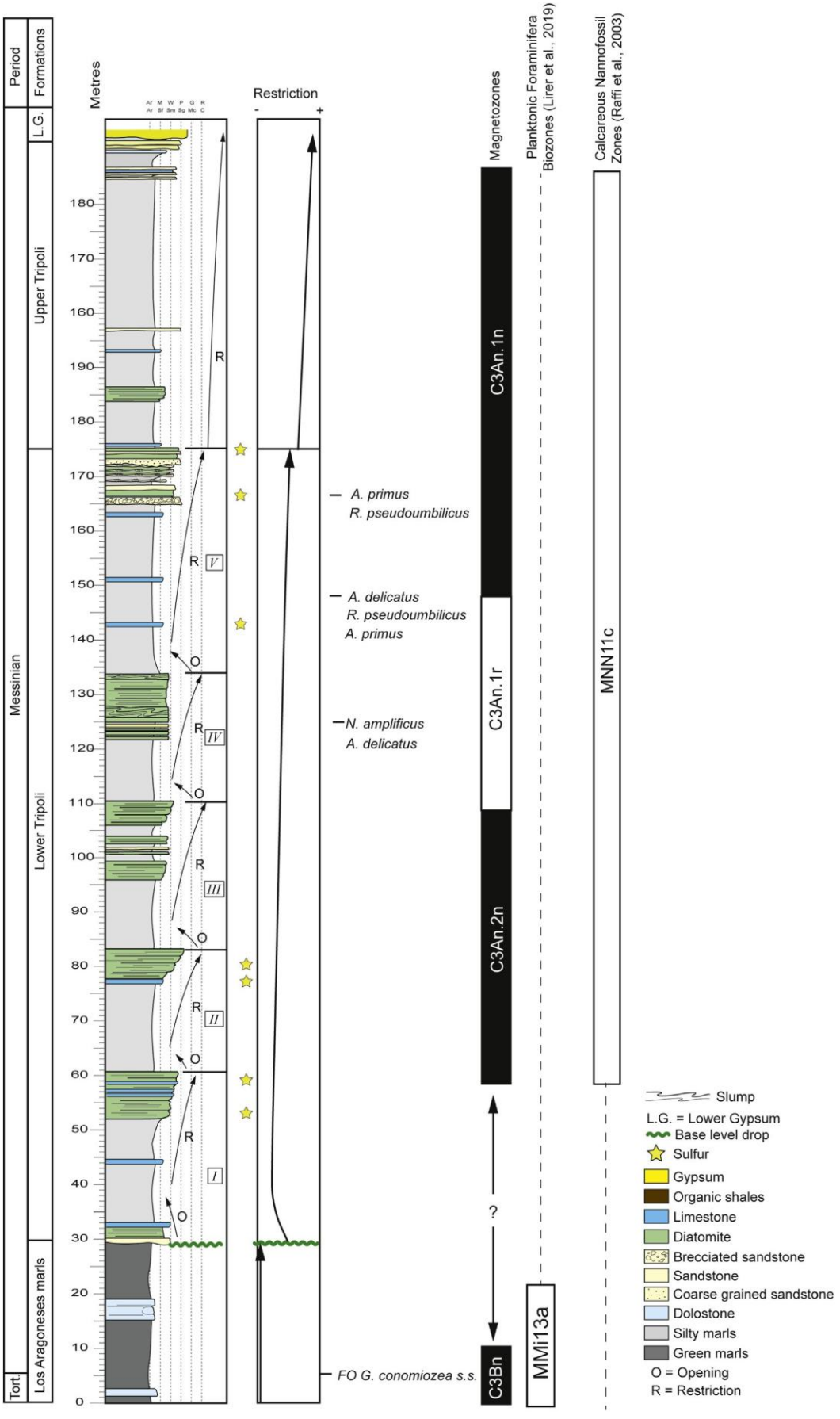
Period
Formations
L.G.
Messinian
Tort.
Upper Tripoli
Lower Tripoli
Los Aragoneses marls
Metres
Ar M W P G R
Ar Bf Bm Bu Mc C
Restriction
- +
R
O
I
II
III
IV
V
A. primus
R. pseudoumbilicus
A. delicatus
R. pseudoumbilicus
A. primus
N. amplificus
A. delicatus
FO G. conomiozea s.s.
Magnetozones
C3An.1n
C3An.1r
C3An.2n
C3Bn
?
Planktonic Foraminifera Biozones (Lirer et al., 2019)
MMi13a
Calcareous Nannofossil Zones (Raffi et al., 2003)
MNN11c
Slump
L.G. = Lower Gypsum
Base level drop
Sulfur
Gypsum
Organic shales
Limestone
Diatomite
Brecciated sandstone
Sandstone
Coarse grained sandstone
Dolostone
Silty marls
Green marls
O = Opening
R = Restriction

Fig. 13. Sedimentological log of the Serrata section with possible magnetozones, high frequency (I to V) and long-term opening-restriction cycles.

basin restrictions. This is also suggested by the occurrence of evaporites in subaqueous or sebkha environments on the eastern margin. In front of the Gilbert delta, during restricted periods, the mixing of marine and freshwaters was not favorable to the precipitation of evaporites but a salinity gradient certainly existed further east. In addition, oxygen-depleted bottom conditions developed during the deposition of the Lower Tripoli Fm in hypersaline conditions as indicated by the lack of bioturbations, the high organic content, the precipitation of gypsum, the intense activity of the bacterial sulphate reduction, and the significance of the organic markers (Russell et al., 1997; Rouchy et al., 1998). Recently Andreetto et al. (2019) interpreted these data as being indicative of a stratification of the water column. Nevertheless, marine conditions persisted during the deposition of the entire Lower Tripoli Fm (Rouchy et al., 1998).

The Messinian age of the Terminal Limestones grading basinward to diatom-bearing marls suggests that they are partly coeval with the Lower Tripoli Fm of the Serrata area. The Terminal Limestones Mbr was deposited during the onset of the fifth high frequency cycle described by Wrobel and Michalzik (1999) and during a rise in baselevel as attested by the onlap geometry on the Los Cautivos Fm

(Fig. 14E). This flooding induced an attenuation of restricted conditions in the whole basin. We interpret the thick marl interval at the base of the fifth cycle in the Lower Tripoli Fm as an indication of a more important reopening compared with the previous cycles I to IV. This last restoration of open marine conditions is inferred to be coeval with the marine reflooding recorded by the onlap of Terminal Limestones in the Los Cautivos area.

A second major drop in base-level is recorded by the S2 surface and a rapid basinward shift of depositional environments. In the Los Monteros area, the sharp transition from carbonate slope environment to conglomeratic submarine channel infill on both sides of S2 suggests a forced regression during a base-level drop. In this area, the lack of indications of subaerial exposure below S2 suggests that the surface formed in a subaqueous environment. Incisions on the upper carbonate slope fed the coarse-grained submarine fan delta deposits observed in the Las Ruzafas area. These deposits show a limited lateral distribution because of their transport as traction carpet in the inertia-flow layer (Postma et al., 1988; Prior and Bornhold, 1989, 1990). In this area, erosion and collapse of the western margin during the relative base-level fall are recorded by the occurrence of olistoliths embedded in the MC Mbr and by slump scars sealed by conglomerates or marls of the overlying members (Fig. 14F). On the southeastern margin, this base-level drop was also recorded by the S2 surface between the Terminal Limestones and overlying alluvial fan deposits of the MC Mbr in the Barranco El Rayo area, between offshore marls and coarse-grained fan delta deposits in the Los Batanes area and between diatom-bearing marls of the Tripoli Fm and wave-modified sandstones in the El Consejero area. The occurrence of reworked Tarbellastrea pebbles in Los Batanes indicates that older carbonate platforms on the basin margins were eroded and probably exposed during the deposition of the MC Mbr. On this margin, conglomeratic fans delta deposits grade basinward over short distances to fine or medium grained sandstones transported further away than pebbles in turbulent suspension clouds. The presence of feeding channels and coarse-grained submarine fan delta deposits in the western part of the basin and only sandy facies devoid of basement pebbles between Los Arcos and El Consejero indicates that the siliciclastic material was mainly provided by the western margin. This unit is correlated in the Serrata with sandy turbidites and conglomeratic beds at the top of the Lower Tripoli Fm.

The base-level drop continued with the deposition of the Upper Tripoli Fm pinching out southwestward and characterised by the disappearance of autochtonous marine fauna, the disappearance of marine diatoms, an increase in siliciclastics, and a drastic increase in freshwater inputs (Benali et al., 1995; Rouchy et al., 1998). This evolution indicates an increasing continentalisation of the basin and the transition toward endorheic conditions (Benali et al., 1995; Jurkschat et al., 2000; Garcia-Veigas et al., 2019). The pinch-out of the Upper Tripoli Fm toward the southwest over a short distance suggests that a tectonic event generated a compartmentalisation of the basin during the second base-level drop and an activity of the FCCL fault cannot be excluded in this context.

Salina and sebkha facies of the Lower Gypsum Fm pinch out and onlap westward on the roof of the MC Mbr in the Los Batanes area (Fig. 14F). In the Serrata area, the sharp contact between the Upper Tripoli Fm and the Lower Gypsum Mbr is in accordance with a rapid and drastic confinement of the basin. However regular incursions of marine waters occurred over or through the sill that was probably formed by the Tercia ridge (see Section 6.2) to allow the precipitation of the consistent volume of evaporites of the Lower Gypsum (Ayora et al., 1994). The evaporites are not Tortonian as they postdate the Tripoli Fm that has been dated to the Messinian on the basis of nannofossils and foraminifera. Thus, they are Messinian in age since no Pliocene deposits were identified in the basin. The occurrence of a subaerial exposure surface (S3 surface) materialised by a palaeosoil at the top of the Lower Gypsum in the Los Arcos area and by an incision filled by continental debris flow deposits between Los Arcos and Los Batanes indicates that another drop in base-level occurred after the deposition of this first evaporitic unit (Fig. 14F).

In the Serrata area, megabreccias interpreted as dissolution/collapse features due to karstification were described at the top of the Lower Gypsum (Rouchy et al., 1998). In addition, two boreholes located in the central part of the basin (Fig. 2) crossed a thick halite unit (Orti et al., 1993; Garcia-Veigas et al., 1994). In the Lorca-S4 borehole the evaporitic unit is composed of 200 m-thick halite deposits covered by a only 25 m-thick gypsum unit (Garcia-Veigas et al., 1994). As a consequence and as envisaged by Rouchy et al. (1998) and Garcia-Veigas et al. (2019), the halite unit is certainly a lateral equivalent of a part of the Lower Gypsum Fm. Halite precipitated first from marine waters in the lower part of the unit and from meteoric waters in the upper part after a gradual closing of the basin and its desiccation (Ayora et al., 1994; Garcia-Veigas et al., 1995, 2019). This suggests that the surface of subaerial exposure at the top of the Lower Gypsum on margins is coeval with the deposition of the younger halite deposits in the deepest parts of the basin when it was disconnected from marine waters. The exposure also indicates that the drop in base-level continued after deposition of the first massive evaporites units. Lowstand deposits coeval with the exposure certainly exist outside the Lorca Basin. The subaerial exposure of the western margin during this major drop in base-level is marked by the presence of root traces below the incision surface S3 that eroded the Terminal Limestones Mbr and the older Los Cautivos Conglomerates. In the Los Cautivos area the S2 surface is not preserved below the S3 surface.

After this last major base-level drop, a new rise in base-level is indicated by the deposition of the Upper Gypsum Fm (Fig. 14G) showing an onlap of evaporitic marls on the S3 surface in the southern part of the basin. However, the intercalation of scarce salina and sebkha facies with desiccation cracks within marls indicates the occurrence of periods of hypersaline conditions and short-lived subaerial exposures during this period of unstable rise in base-level. Subsequently, marine waters reentered the basin and marine conditions prevailed in the lower part of the Cañada Honda Fm marked by the deposition of wavedominated sandstones and marine conglomerates. In the Las Ruzafas area slope failures ceased before the development of braided river deposits overlying the S3 surface. The vertical transition from braided river conglomerates above the S3 surface to marls of the MM Mbr, which were deposited in a brackish environment because of the vicinity of alluvial fans and freshwater inputs, indicates a backstepping of depositional environments after the major lowering of base-level

recorded by the S3 surface. In the Los Cautivos and Los Monteros areas the onlap of alluvial fan deposits of the AC Mbr on the S3 surface attests of a renewal in the creation of accommodation space after a major drop in base-level.

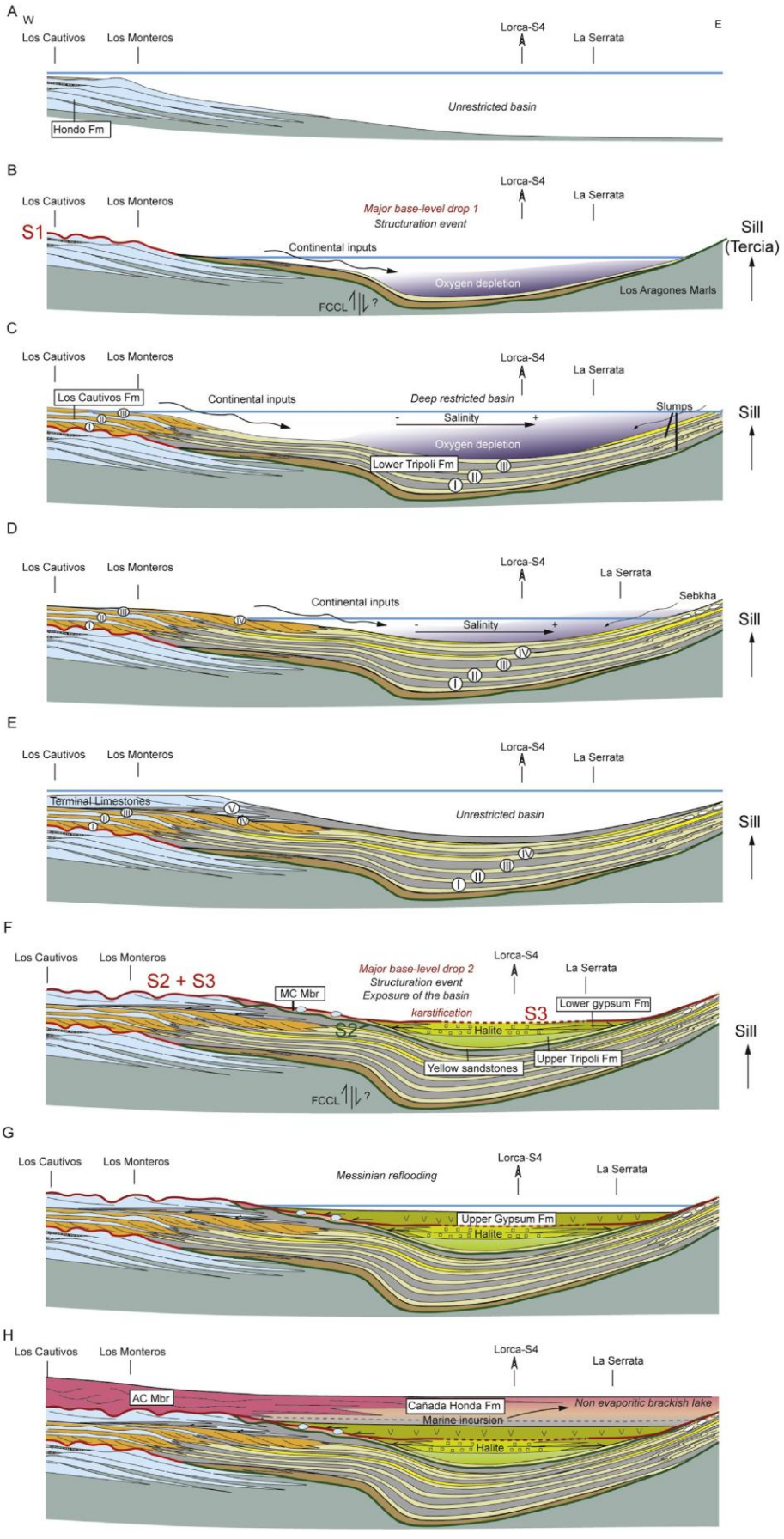
A
W
E
Los Cautivos
Los Monteros
Lorca-S4
La Serrata
Unrestricted basin
Hondo Fm
B
Major base-level drop 1
Structuration event
S1
Continental inputs
Oxygen depletion
Los Aragones Marls
FCCL
Sill
(Tercia)
C
Los Cautivos Fm
Deep restricted basin
Salinity
Slumps
Lower Tripoli Fm
Sill
D
Sebkha
Sill
E
Terminal Limestones
Unrestricted basin
Sill
F
S2 + S3
MC Mbr
Major base-level drop 2
Structuration event
Exposure of the basin
karstification
S3
S2
Halite
Lower gypsum Fm
Upper Tripoli Fm
Yellow sandstones
FCCL
Sill
G
Messinian reflooding
Upper Gypsum Fm
Halite
H
AC Mbr
Cañada Honda Fm
Non evaporitic brackish lake
Marine incursion
Halite

Fig. 14. Sedimentary and stratigraphical evolution of the Lorca Basin during the Late Tortonian and the Messinian.

During the highstand progradation of alluvial fan systems of the AC Mbr and the deposition of the upper part of the Cañada Honda Fm, the marine waters were gradually diluted by freshwater carried from the hinterland and a shallow brackish lake devoid of evaporites formed in the whole basin (Fig. 14H). Such a depositional environment is similar to the Lago Mare facies described in many marginal basins all around the Mediterranean basin (Rouchy et al., 2001; Aguirre and Sanchez-Almazo, 2004; Clauzon et al., 2005; Cosentino et al., 2005; Orszag-Sperber, 2006). The important terrigenous inputs from the western margin under a humid climate compensated and exceeded gradually the accommodation space and prograding alluvial and lacustrine deposits finally covered brackish deposits. The gradual enrichment in flood-related deposits and the appearance of fluvial channels in the upper part of the formation are in accordance with a prograding trend.

6.2. Controls on sedimentary cycles

Several authors tentatively proposed correlations between eccentricity cycles and the onset of the salinity crisis on the basis of magnetostratigraphical dating (Krijgsman et al., 1999; Hilgen et al., 2007). They proposed that long-term orbital cycle forcing superimposed onto tectonics controlled the appearance of evaporites. The occurrence of a significant base-level fall prior to the deposition of evaporites in marginal basins is discussed as for example in the Sorbas Basin (Braga and Martin, 1996; Bourillot et al., 2009, 2010; Manzi et al., 2013). Our field observations show that in the Lorca Basin several base-level drops predated the deposition of the Lower Gypsum Fm. These base-level drops are compared with the major changes observed in the Cenozoic sea-level curve from the Late Tortonian to the Pliocene (Fig. 15). Haq et al. (1987), Abreu and Anderson (1998) and Miller et al. (2011) all consider two main sea-level falls during the Messinian despite their different timing (Fig. 15A). Major sedimentary cycles observed in the Lorca Basin can be tentatively correlated with the accommodation curve deduced from the global sea-level curve of Miller et al. (2011) and corrected by local uplift or subsidence (Fig. 15B). The two main base-level drops associated with S1 and S2/S3 surfaces can be correlated with eustatic falls at −6.8 or -6.5 Ma and at about −6 Ma respectively. The occurrence of N. amplificus (6.94–5.94 Ma; Gradstein et al., 2012) in the middle part of the Lower Tripoli Fm indicates that the second base level-drop that predated the deposition of the Upper Tripoli and the Lower Gypsum occurred after −6.9 Ma. The first occurrence of N. amplificus is located in the uppermost part of the magnetozone C3Ar (Raffi et al., 2006). However, in the Serrata section, N. amplificus occurs in the lower part of an interval of reversed polarity defined by Krijgsman et al. (2000). Consequently, the reversed-polarity interval in the Serrata section is probably the younger magnetozone C3An.1r between −6.4 and −6.25 Ma. In this case, an age of about −6 Ma for the onset of deposition of the Lower Gypsum cannot be ruled out. The final base-level drop (S3 surface) that resulted in subaerial exposure of the Lorca Basin was probably also enhanced by the local lowering of relative sea-level due to evaporation of enclosed Mediterranean marine waters after the closure of the Gibraltar strait and the disappearance of perennial connections between Atlantic and Mediterranean domains (Duggen et al., 2003; Jolivet et al., 2006; Garcia-Castellanos et al., 2009; Manzi et al., 2013; Roveri et al., 2014a).

A superimposed tectonic activity certainly controlled the amplitude of eustasy-related variations in accommodation space. In the model of Montenat and Ott d'Estevou (1999), the Tercia ridge corresponds to a drag fold formed during the Late Tortonian and a syncline occurred in the Serrata area because of the transpressive deformation in the vicinity of the strike-slip Alhama de Murcia fault system. However, during the Late Tortonian, the lack of basin restriction, the dominance of terrigenous inputs from the External Betics, and the lack of evidence of

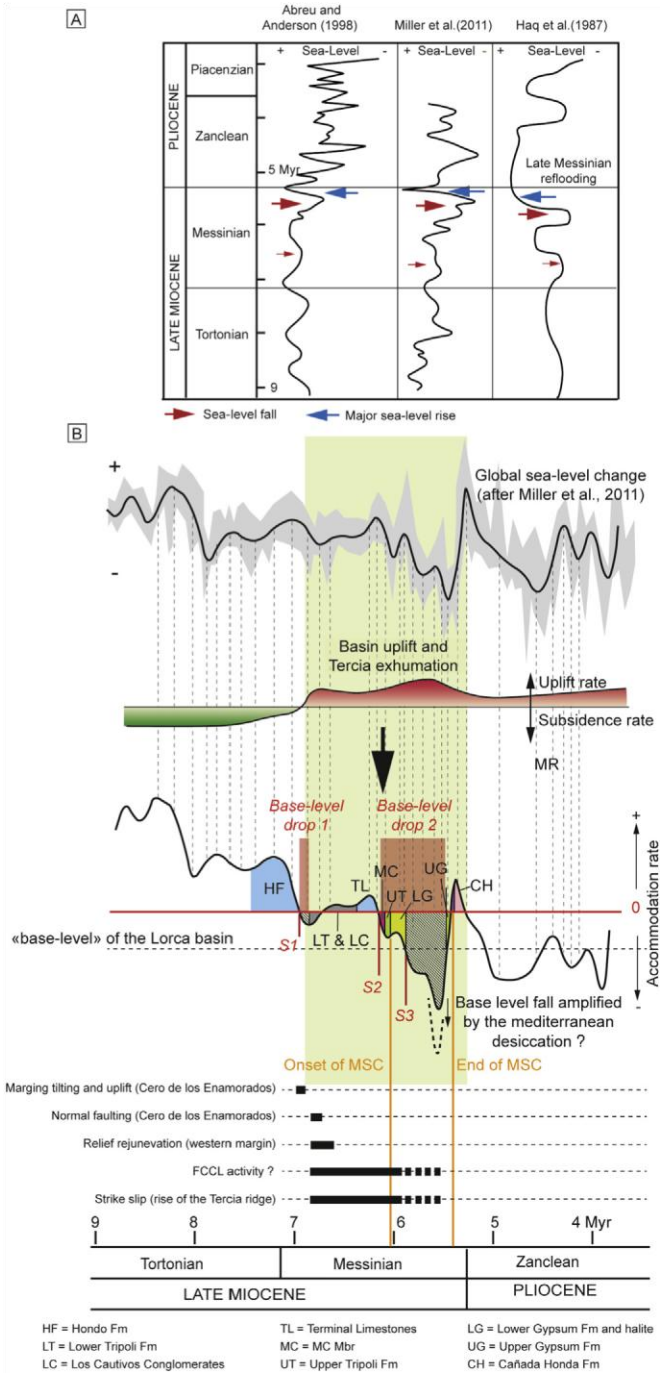

Fig. 15. Sedimentary evolution, eustasy, and the structural framework of the Lorca Basin during the Late Tortonian and the Messinian.

terrigenous inputs from the Tercia ridge actually located less than 2.5 km from the Serrata suggest that this massif was not yet exhumed and therefore did not act as a sill. In contrast, a folding or tilting of the southeastern margin may have occurred from the Late Tortonian to Early Messinian as suggested by the gradual pinch-out of the Hondo Fm on top of the Parilla Fm in the area of the Cejo de los Enamorados. In addition, the occurrence of slumps showing a westward displacement in diatomites indicates that a slope was present in the Serrata area during the Messinian. A shallow water or exposed high in the eastern margin is deduced by the slope orientation and the gravitydriven sandstones at the top of the Lower Tripoli Fm showing N310° palaeoflow directions. The sliding direction of slumps in diatomites suggests that a possible origin of gravity-driven deposits in this part of the basin is related to a steepening of the eastern margin. Such slope modifications probably occurred during the exhumation of the Tercia ridge related to the strike-slip activity of the Alhama de Murcia fault system during the uplift of the Betics (Booth-Rea et al., 2002) (Fig. 15B). By considering an exhumation of the Tercia ridge during the Messinian, this high probably acted as a sill and favoured basin restrictions during low accommodation space periods. Subsequently, the Tercia ridge continued to act as a sill during the deposition of Messinian evaporites.

In addition, Gilbert delta systems occur generally in tectonically active zones with a stepped margin and an abrupt transition from shallow or subaerial environments to a deep basin (Postma, 1990; Garcia-Garcia et al., 2006a, 2006b; Alçiçek, 2007; Breda et al., 2007; Backert et al., 2010). The transition from a

coral-rich carbonate platform of the Hondo Fm to the Gilbert delta of the Los Cautivos Fm suggests that a major structural event and a rejuvenation of reliefs coeval with the appearance of a stepped margin occurred at the beginning of the Messinian (Fig. 15B). This timing is in accordance with the scenario of a growth of the Tercia ridge during the Messinian as proposed by Martinez-Diaz (2002) and Meijninger and Vissers (2006) and with a major structural reorganisation associated with a regional uplift (Jolivet et al., 2006; Pedrera et al., 2006; Iribarren et al., 2007, 2009; Augier et al., 2013). This regional uplift was induced by the inversion of the Algero-Balearic Basin (Jolivet et al., 2006; Giaconia et al., 2015; Do Couto et al., 2016) and amplified the eustasy-related decrease in accommodation space and limited the amplitude of reflooding as envisioned in numerous marginal basins of the Mediterranean domain (Roveri and Manzi, 2006; Roveri et al., 2014b) (Fig. 15B). Finally, during the Late Messinian, the renewal in accommodation and the short-lived marine incursion (base of the Cañada Honda Fm) are coeval with an eustatic rise and with a decrease in the intensity of compressional deformation and uplift (Carnevale et al., 2006; Bache, 2012; Roveri et al., 2014a) (Fig. 15B). Pliocene deposits have not been identified in the Lorca Basin. This suggests that an important regional uplift either compensated the eustatic rise during the Pliocene or generated the erosion of marine deposits after the Pliocene flooding.

In this context of regional uplift, a local structural control on high frequency sedimentary cycles can be postulated for the Lorca Basin. The reflooding of incised valleys by the diatomites of the Tripoli Fm on the toe of the Cejo de los Enamorados is coeval with synsedimentary faulting that locally enhanced the increase in accommodation (Fig. 9). In the Los Cautivos Fm, the occurrence of periods of pure progradation and associated forced regression indicates that high frequency aggradation/backstepping/progradation cycles (I to IV cycles) were mainly controlled by variations in accommodation rather than by variations in the sedimentary flux. A eustatic control on these high frequency cycles was not excluded by Wrobel and Michalzik (1999) who interpreted them as 4th order cycles. In addition, Rouchy et al. (1998) argued that restriction/opening cycles in the Lower Tripoli Fm were due to global sea-level fluctuations rather than to tectonic processes because of the short duration of cycles. However, several studies show that high frequency cycles sometimes less than 10 Kyr in duration in Gilbert delta systems can be directly controlled by the synsedimentary activity on marginal faults (Gupta et al., 1999; Mortimer et al., 2005; GarciaGarcia et al., 2006a, 2006b). A synsedimentary activity could have generated a partitioning of the basin with an eastern subsiding and confined area and a less subsiding western part (Guillen Mondejar et al., 1995; Meijninger and Vissers, 2006). In this context an activity of the FCCL can be envisioned as proposed by Guillen Mondejar et al. (1995).

6.3. The Lorca Basin in the western Mediterranean context

On the basis of the Messinian age of the pre-evaporitic units in the Lorca Basin, a reflection on correlations with other Neogene basins of the Betics can be made, even if further biostratigraphical investigations in the Lorca Basin will be necessary for more precise calibrations. The large distribution of diatom-bearing deposits in the Mediterranean domain prior to evaporites is interpreted as the first evidence of basin restriction associated to a base-level drop (Blanc-Valleron et al., 2002; Roveri et al., 2014a; Pellegrino et al., 2018). However, this event is diachronous and occurred between 7.15 Ma and 6 Ma across different basins (Hilgen and Krijgsman, 1999; Roger et al., 2000; Blanc-Valleron et al., 2002; Rouchy and Caruso, 2006; Orszag-Sperber et al., 2009; Roveri et al., 2014a; Pellegrino et al., 2018). These variations can be interpreted in terms of local changes of the local hydrology that controls the availability of nutrients and the physico-chemical parameters of the water column. However, tectonic activity probably also played an important role as it can control the local onset of basin restriction in areas of important tectonic activity such as the Betics. Because of their more internal location, the Guadix and Granada basins recorded a marine to continental transition at the end of the Tortonian (RodríguezFernández and de Galdeano, 2006; Pla-Pueyo et al., 2009). In the neighbouring Fortuna Basin, the first occurrence of evaporites is dated as Tortonian (Lancis et al., 2010) (Fig. 16A). It corresponds to the Lower Gypsum overlain by the marine Sanel Marls. The TortonianMessinian boundary was placed by Lancis et al. (2010) at the top of these marls and just below the overlying Tale Gypsum. This discrepancy in age of gypsum deposits between the Lorca and Fortuna basins suggests that the first restriction phase coeval with the deposition of the Lower Gypsum in the Fortuna Basin during the Tortonian predated the first restriction in the Lower Tripoli of the Lorca Basin. The Tale Gypsum is overlain by the Chicamo Cycles characterised by diatombearing marls with intercalated evaporites. However the first occurrence of N. amplificus at ~6.9 Ma is located at the topmost of the Chicamo Cycles below the Wichmann Conglomerates in the Fortuna Basin, while N. amplificus is present below the Lower Gypsum Fm in the Lorca Basin (Fig. 16A). A subaerial exposure occurred at the top of the Wichmann Conglomerates (Santisteban and Taberner, 1983) and this erosional event can be correlated with the first erosional surface S1 in the Lorca Basin. However a precise dating of the base of the Lower Tripoli Fm should be performed to validate such a correlation. The magnetozone C3An.1r probably located in the marine Lower Tripoli Fm in the Lorca Basin was placed in the lacustrine deposits of the Rambla Salada Gypsum above the marine-continental transition located at the top of the Wichmann Conglomerates (Lancis et al., 2010) (Fig. 16A). The short marine event at the base of the Cañada Honda Fm in the Lorca Basin was not recorded in the Fortuna Basin where deposits are continental from the Wichmann Conglomerates to the Messinian-Pliocene boundary. All these features suggest that the Fortuna Basin became restricted and recorded the transition to continental environments before the Lorca Basin. Local tectonic control linked to the transalboran strike-slip faults is probably responsible for the diachronous evolution of these two basins.

In the Nijar and Sorbas basins, the onset of diatom-rich sedimentation occurred during the Messinian after a major uplift along strikeslip faults near the Tortonian-Messinian boundary (Pedrera et al., 2006; Bourillot et al., 2010; Do Couto et al., 2014). In these basins, transgressive uppermost Tortonian carbonates of the Azagador Mbr onlap basement rocks or tilted Tortonian turbidites (Fig. 16B). In the Sorbas Basin a second angular unconformity due to the uplift of the southern basin margin exists between these Tortonian carbonates and the overlying Messinian Bioherm Unit (Martin and Braga, 1996). This Messinian event marks the onset of the diatom-rich sedimentation of the Abad Fm (Braga and Martin, 1996; Bourillot et al., 2010). This unconformity is not recorded in northern and eastern Mediterranean basins. However, an erosional surface (S1) was also observed in the Lorca Basin at the base of the diatom-bearing deposits of the Lower Tripoli Fm. This suggests that local tectonics probably controlled this first erosional event and the uplift of the Betics coeval with the appearance of structural highs during the Messinian favoured the first basin restriction observed in the Lorca Basin.

A reopening prior to the salinity crisis is documented by carbonates of the Terminal Limestones in the Lorca Basin (Fig. 16). Similar Poritesrich carbonates of the

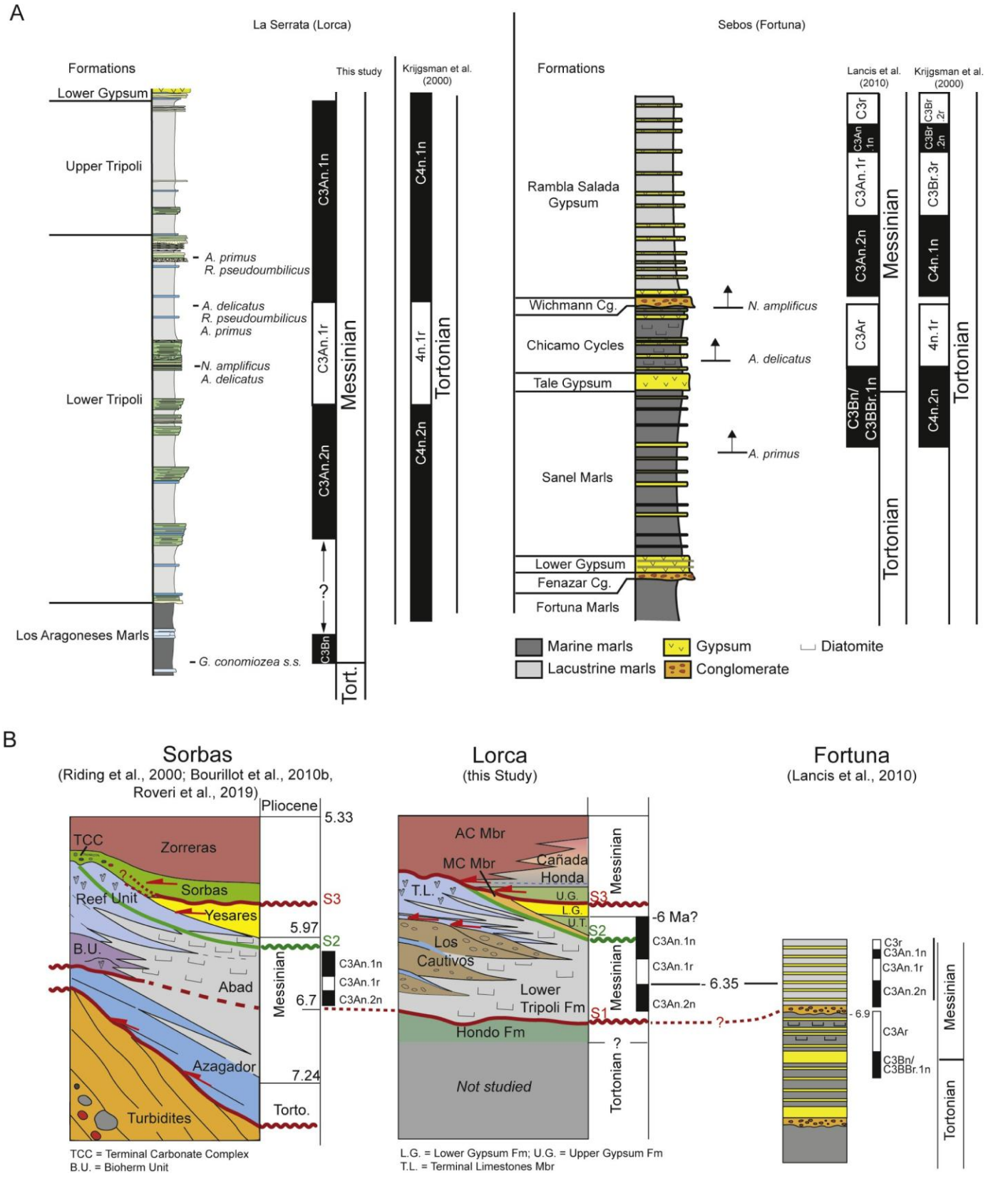

Fig. 16. Correlations of the main Messinian surfaces between the Sorbas Basin, the Lorca Basin, and the Fortuna Basin.

Reef Unit occur in the Sorbas Basin (Brachert et al., 1996; Braga and Aguirre, 2001; Martin et al., 2010). In this basin the developpement of the Reef Unit started at the base of the magnetozone 3An.1n (Bourillot et al., 2010). In the Lorca Basin, the age of the Terminal Limestones cannot be determined with precision. However if, as discussed above, the reversed-polarity magnetozone in the Lower Tripoli Fm is consistent with the magnetozone C3An.1r, the upper part of the

Lower Tripoli and the Terminal Limestones were deposited during the magnetozone 3An.1n at the same time than the Reef Unit in Sorbas. The transgression allowed the carbonates to cover uplifted Sierra Alhamilla separating the Sorbas and the Nijar basins (Sánchez-Almazo et al., 2001). The coeval installation of Porites-rich carbonates in several basins of southern Spain and all around the Mediterranean basin (Cornée et al., 2004) reinforces the idea that the flooding was linked to a global base-level rise that restored connections between subbasins. The monogeneric signature of Messinian reefs is explained by a general cooling of surface sea-waters during the northward migration of the African plate (Bosellini and Perrin, 2008; Perrin and Bosellini, 2013).

The second base-level drop is illustrated by the erosional surface S2 (Fig. 16B). In the Sorbas and Nijar basins, forced regression geometries in carbonates are documented (Martin and Braga, 1996; Warrlich et al., 2005; Sánchez-Almazo et al., 2007). As a consequence in these basins, as in the Lorca Basin, the last Messinian Porites-rich carbonates recorded a base-level drop prior to the onset of the salinity crisis. If as proposed, the magnetozones of the Lower Tripoli Fm and the diatombearing Abad Fm in Sorbas are similar, relative sea-level falls in the Nijar, Sorbas and Lorca basins can be coeval and an equivalent of the S2 surface is present within Porites carbonates (Fig. 16B). In the Lorca Basin, the development of coarse-grained fan delta deposits after the base-level drop was probably due to the more internal location of the basin compared with the Nijar and Sorbas basins where the carbonate production continued during the forced regression. In the Lorca Basin no evidence of an incision surface or prolonged subaerial exposure exists at the base of the Lower Gypsum but a subaerial exposure (S3 surface) exists on top of the formation and on basin margins. This indicates that evaporites in the Lorca Basin were deposited during a gradual drying and before an exposure of the basin as proposed by Rouchy and Caruso (2006) rather than during a reflooding after an exposure of the basin as envisioned by Riding et al. (1998) and Braga et al. (2006) in the Sorbas Basin. It is worth noting that in the latter basin no time gap was identified between diatomites and overlying gypsum (Manzi et al., 2013).

A surface of subaerial exposure was described in the Sorbas Basin at the top of evaporites (Bourillot et al., 2010; Clauzon et al., 2015; Do Couto et al., 2015) (Fig. 16B), the Nijar Basin (Fortuin and Krijgsman, 2003; Omodeo-Salé et al., 2012) and in Morocco (Cornée et al., 2016). Even if the model of Roveri et al. (2008, 2014b) is mainly based on the stratigraphy of Apennine and Sicilian domains and its generalisation to the wide deep Mediterranean domain can be questioned, we interpret the entire exposure of the Lorca Basin as coeval with the deposition of lower evaporites and halite in the deep Mediterranean basin. Such a scenario was already proposed for several circum-Mediterranean margins (Clauzon et al., 2005; Roveri et al., 2008, 2014b; Ryan, 2009; Lugli et al., 2015). Maillard et al. (2006) and Maillard and Mauffret (2006) consider that this event led to the entire exposure of the Central Valencia Basin while evaporites accumulated in the Provençal Basin. Roveri et al. (2008) and Manzi et al. (2013) proposed that marginal evaporites were reworked during the exposure and resedimented in the deep Mediterranean domain prior to the deposition of a massive halite unit. However, the configuration of the Mediterranean Basin and the amplitude of the final drawdown is still debated as some authors consider a limited amplitude of the base-level drop (Hardie and Lowenstein, 2004; Lugli et al., 2015; Cornée et al., 2016) and sporadic to permanent connections with the Atlantic domain (Krijgsman and Meijer, 2008; Stefano et al., 2010; Merzeraud et al., 2019) while other propose a sea-level drop of several hundred to more than one thousand m (Hsü, 1973; Lofi et al., 2005; Urgeles et al., 2011; Madof et al., 2019). The lack of deep incisions in the Lorca Basin is more in accordance with a limited drawdown. The surface of subaerial exposure at the top of the Terminal Limestones in the western part of the Lorca Basin records an important time gap of probably more than 0.5 Ma from the beginning of the base-level drop at the base of the MC Mbr, to the deposition of brackish marls of the MM Mbr.

In the Lorca Basin, as in some other peri-Mediterranean basins and in many large evaporitic systems, the end of the evaporitic episodes is marked by the last evaporitic sequences and the post evaporitic deposits such as the Lago-Mare displaying an onlapping geometry. This onlap is commonly associated to the deposition of “Lago Mare type” facies of shallow brackish lake environment (Upper Gypsum Fm) (Fig. 16B). A similar onlap geometry of Upper evaporites was observed in the Valencia Basin and in the whole Mediterranean Basin. For several authors, the Lago Mare facies are related to a generalised reflooding at the Mediterranean scale and correspond to the restoration of connections with the Paratethys (Do Couto et al., 2014; Popescu et al., 2015; Marzocchi et al., 2016; Stoica et al., 2016). Conversely, a considerable number of studies provide evidence of an abrupt restoration of open marine conditions at the onset of the Zanclean putting an end to the restricted, brackish to lacustrine conditions of the late Messinian (Pierre et al., 2006; Caruso et al., 2020; Garcia-Castellanos et al., 2020; and references therein). This does not preclude that marine influences may have been only temporarily restored in some basins. From a study of the ostracod content, De Decker et al. (1988) concluded to the undisputable continental aspect of the Lago-Mare, with only one exception marked by some marine affinity just above the uppermost gypsum layer. This may explain the short-lived marine incursion that occurred in the lower part of the Cañada Honda Fm in the Lorca Basin. The transition to lacustrine environments occurred in the upper part of the Cañada Honda Fm as a result of high terrigenous and freshwater inputs. In the Sorbas Basin the spatiotemporal relationship between the marine deposits of the TCC on basin margins and the subaerial exposure at the top of the Yesares gypsum is still debated (Cornée et al., 2004; Bourillot et al., 2010; Roveri et al., 2019). Nevertheless, in the central part of the basin shallow marine conditions could have been restored during the Late Messinian leading to the deposition of the Sorbas Mbr (Bourillot et al., 2010, Roveri et al., 2019). Marine deposits were also gradually replaced by the terrestrial Zorreras Mbr (Roep et al., 1998).

7. Conclusions

A consistent geological framework is proposed for the Lorca Basin with respect to neighbouring Neogene basins and the western Mediterranean domain during the Late Miocene. The proposed scenario is strongly rooted on updated micropalaeontological dating. The Messinian age of evaporites of the Lorca Basin is consistent with ages of gypsum deposits in the Sorbas or Nijar basins. This age indicates that, apart the more proximal Granada, Guadix, and Fortuna basins that experienced a marinecontinental transition during the Late Tortonian or the Early Messinian, the salinity crisis was probably synchronous in most Neogene basins of southern Spain. No Tortonian salinity crisis occurred in the Lorca Basin even if the first evaporites associated with diatom-bearing deposits precipitated probably earlier during the Messinian in the Lorca Basin than in some other basins of the Betic Cordillera. Several stages of base-level fall associated with basin restriction and reflooding are correlated with eustatic lowering of base-level and were amplified by regional uplift during the onset of the transpressive motion along trans-Alboran fault systems. Sedimentary features suggest that the exhumation the Tercia ridge occurred during the Early Messinian. This high acted as a sill during the successive restriction phases. Evaporites of the Lorca Basin were deposited during the Messinian during a gradual lowering of base-level while the Lower evaporites in the deep Mediterranean domain formed during the entire draining of the marginal basins. The Upper evaporites and the brackish Lago Mare facies extended in the Lorca Basin during the Late Messininan and a short-lived marine incursion occurred just above the last gypsum layers.

Aknowledgements

We are grateful to the CNRS-INSU (Centre National de la Recherche Scientifique – Institut National des Sciences de l'Univers) as part of the SYSTER (Sytème Terre: processus et couplages) action. We thank Catherine Chagué, Jesus M. Soria and the anonymous reviewer for their comments, advices, and corrections that helped improve the quality of the manuscript. We are grateful to Mary Ford for correcting the English. We also thank Gregorio Francisco Martinez Rodriguez for his material and logistical help during field missions and Aurélien Eglinger for his company in the field and his role as scale on some images.

References

Abreu, V., Anderson, J., 1998. Glacial eustasy during the Cenozoic: sequence stratigraphic implications. AAPG Bull. 82, 1385–1400.

Aguirre, J., Sanchez-Almazo, I., 2004. The Messinian post-evaporitic deposits of the Gafares area (Almeria-Nijar basin, SE Spain). A new view of the "Lago-Mare" facies. Sediment. Geol. 168, 71–95.

Alçiçek, M.C., 2007. Tectonic development of an orogen-top rift recorded by its terrestrial sedimentation pattern: the Neogene Eşen Basin of southwestern Anatolia, Turkey. Sediment. Geol. 200, 117–140.

Allen, J., 1963. The classification of cross-stratified units, with notes on their origin. Sedimentology 2, 93–114.

Alsharhan, A.S., Kendall, C.G.St.C., 2003. Holocene coastal carbonates and evaporites of the southern Arabian Gulf and their ancient analogues. Earth Sci. Rev. 61, 191–243.

Anderson, R., Dean, W., 1988. Lacustrine varve formation through time. Palaeogeogr. Palaeoclimatol. Palaeoecol. 62, 215–235.

Andreetto, F., Dela Pierre, F., Gibert, L., Natalicchio, M., Ferrando, S., 2019. Potential fossilized sulfide-oxidizing bacteria in the Upper Miocene sulfur-bearing limestones from the Lorca Basin (SE Spain): Paleoenvironmental implications. Front. Microbiol. 10. https://doi.org/10.3389/fmicb.2019.01031.

Augier, R., Jolivet, L., Do Couto, D., Negro, F., 2013. From ductile to brittle, late- to postorogenic evolution of the Betic Cordillera: Structural insights from the northeastern Internal zones. Bull. Soc. Geol. Fr. 184, 405–425.

Ayora, C., Garcia-Veigas, J., Pueyo, J.J., 1994. X-ray microanalysis of fluid inclusions and its application to the geochemical modeling of evaporite basins. Geochim. Cosmochim. Acta 58, 43–55.

Bąbel, M., 2007. Depositional environments of a salina-type evaporite basin recorded in the Badenian gypsum facies in the northern Carpathian Foredeep. Geol. Soc. Lond., Spec. Publ. 285, 107–142.

Bache, F., 2012. A two step process for the reflooding of the Mediterranean after the Messinian salinity crisis. Basin Res. 24, 125–153.

Backert, N., Ford, M., Malartre, F., 2010. Architecture and sedimentology of the Kerinitis Gilbert-type fan delta, Corinth Rift, Greece. Sedimentology 57, 543–586.

Benali, S., Schreiber, B.C., Helman, M.L., Philp, R.P., 1995. Characterization of organic matter from a restricted/evaporative sedimentary environment: late Miocene of Lorca Basin, southeastern Spain. AAPG Bull. 79, 816–829.

Betzler, C., Braga, J.C., Martin, J., Sanchez-Almazo, I., Lindhorst, S., 2006. Closure of a seaway: stratigraphic record and facies (Guadix basin, Southern Spain). Int. J. Earth Sci. 95, 903–910.

Blanc-Valleron, M.M., Pierre, C., Caulet, J.P., Caruso, A., Rouchy, J.M., Cespuglio, G., Sprovieri, R., Pestrea, S., Di Stefano, E., 2002. Sedimentary, stable isotope and micropaleontological records of paleoceanographic change in the Messinian Tripoli Formation (Sicily, Italy). Palaeogeogr. Palaeoclimatol. Palaeoecol. 185, 255–286.

Blankenship, C., 1992. Structure and palaeogeography of the External Betic Cordillera, southern Spain. Mar. Pet. Geol. 9, 257–264.

Bøe, R., Bugge, T., Rise, L., Eidnes, G., Eide, A., Mauring, E., 2003. Erosional channel incision and the origin of large sediment waves in Trondheimsfjorden, central Norway. GeoMar. Lett. 24, 225–240.

Booth-Rea, G., Garcia-Duenas, V., Azanon, J.M., 2002. Extensional attenuation of the Malaguide and Alpujarride thrust sheets in a segment of the Alboran basin folded during the Tortonian (Lorca area, Eastern Betics). C. R. Geosci. 334, 557–563.

Booth-Rea, G., Azanon, J.M., Garcia-Duenas, V., Augier, R., 2003. Uppermost Tortonian to Quaternary depocentre migration related with segmentation of the strike-slip Palomares Fault Zone, Vera Basin (SE Spain). C. R. Geosci. 335, 751–761.

Booth-Rea, G., Azanon, J.M., Garcia-Duenas, V., 2004. Extensional tectonics in the northeastern Betics (SE Spain): case study of extension in a multilayered upper crust with contrasting rheologies. J. Struct. Geol. 26, 2039–2058.

Bosellini, F.R., Perrin, C., 2008. Estimating Mediterranean Oligocene–Miocene sea-surface temperatures: an approach based on coral taxonomic richness. Palaeogeogr. Palaeoclimatol. Palaeoecol. 258, 71–88.

Bourillot, R., Vennin, E., Rouchy, J.M., Durlet, C., Rommevaux, V., Kolodka, C., Knap, F., 2009. Structure and evolution of a Messinian mixed carbonate-siliciclastic platform: the role of evaporites (Sorbas Basin, South-east Spain). Sedimentology 57, 477–512.

Bourillot, R., Vennin, E., Rouchy, J.M., Blanc-Valleron, M.M., Caruso, A., Durlet, C., 2010. The end of the Messinian Salinity Crisis in the western Mediterranean: Insights from the carbonate platforms of south-eastern Spain. Sediment. Geol. 229, 224–253.

Brachert, T., Betzler, C., Braga, J., Martin, J., 1996. Record of climatic change in neritic carbonates: turnover in biogenic associations and depositional modes (Late Miocene, southern Spain). Geol. Rundsch. 85, 327–337.

Brachert, T., Hultzsch, N., Knoerich, A., Krautworst, U., Stückrad, O., 2001. Climatic signatures in shallow-water carbonates: high-resolution stratigraphic markers in structurally controlled carbonate buildups (Late Miocene, southern Spain). Palaeogeogr. Palaeoclimatol. Palaeoecol. 175, 211–237.

Braga, J.C., Aguirre, J.M., 2001. Coralline algal assemblages in upper Neogene reef and temperate carbonates in Southern Spain. Palaeogeogr. Palaeoclimatol. Palaeoecol. 175, 27–41.

Braga, J.C., Martin, J.M., 1996. Geometries of reef advance in response to relative sealevel changes in a Messinian (uppermost Miocene) fringing reef (Cariatiz reef, Sorbas Basin, SE Spain). Sediment. Geol. 107, 61–81.

Braga, J.C., Martin, J.M., Riding, R., Aguirre, J., Sanchez-Almazo, I., Dinarès-Turell, J., 2006. Testing models for the Messinian salinity crisis: the Messinian record in Almería, SE Spain. Sediment. Geol. 188–189, 131–154.

Breda, A., Mellere, D., Massari, F., 2007. Facies and processes in a Gilbert-delta-filled incised valley (Pliocene of Ventimiglia, NW Italy). Sediment. Geol. 200, 31–55.

Buatois, L., Mangano, G., 2004. Animal-substrate interactions in freshwater environments: applications of ichnology in facies and sequence stratigraphic analysis of fluvio-lacustrine successions. In: McIlroy, D. (Ed.), The Application of Lchnology to Palaeoenvironmental and Stratigraphic Analysis. 228. Geological Society, London, Special Publications, pp. 311–333.

Butler, R., Lickorish, W.H., Grasso, M., Pedley, H.M., Ramberti, L., 1995. Tectonics and sequence stratigraphy in Messinian basins, Sicily: Constraints on the initiation and termination of the Mediterranean salinity crisis. Geol. Soc. Am. Bull. 107, 425–439.

Carnevale, G., Landini, W., Sarti, G., 2006. Mare versus Lago-mare: marine fishes and the Mediterranean environment at the end of the Messinian Salinity Crisis. J. Geol. Soc. 163, 75–80.

Caruso, A., Blanc-Valleron, M.M., Da Prato, S., Pierre, C., Rouchy, J.M., 2020. The late Messinian "Lago-Mare" event and the Zanclean Reflooding in the Mediterranean Sea: New insights from the Cuevas del Almanzora section (Vera Basin, SouthEastern Spain). Earth Sci. Rev. 200, 102993.

Catuneanu, O., Abreu, V., Bhattacharya, J.P., Blum, M.D., Dalrymple, R.W., Eriksson, P.G., Fielding, C.R., Fisher, W.L., Galloway, W.E., Gibling, M.R., Giles, K.A., Holbrook, J.M., Jordan, R., Kendall, C.G.St.C., Macurda, B., Martinsen, O.J., Miall, A.D., Neal, J.E., Nummedal, D., Pomar, L., Posamentier, H.W., Pratt, B.R., Sarg, J.F., Shanley, K.W., Steel, R.J., Strasser, A., Tucker, M.E., Winker, C., 2009. Towards the standardization of sequence stratigraphy. Earth Sci. Rev. 92, 1–33.

Chalouan, A., Saji, R., Michard, A., Bally, A., 1997. Neogene tectonic evolution of the southern Alboran basin as inferred from seismic data of Morocco. AAPG Bull. 81, 1161–1184.

Chun, S., Chough, S., 1995. The cretaceous Uhangri Formation, SW Korea: lacustrine margin facies. Sedimentology 42, 293–322.

Clauzon, G., Suc, J.P., Gautier, F., Berger, A., Loutre, M.F., 1996. Alternate interpretation of the Messinian salinity crisis: controversy resolved? Geology 24, 363–366.

Clauzon, G., Suc, J.P., Popescu, S.M., Marunteanu, M., Rubino, J.L., Marinescu, F., Melinte, M. C., 2005. Influence of Mediterranean sea-level changes on the Dacic Basin (Eastern Paratethys) during the late Neogene: the Mediterranean Lago Mare facies deciphered. Basin Res. 17, 437–462.

Clauzon, G., Suc, J.P., Do Couto, D., Jouannic, G., Melinte-Dobrinescu, M.C., Jolivet, L., Quillévéré, F., Lebret, N., Mocochain, L., Popescu, S.M., Martinell, J., Doménech, R., Rubino, J.L., Gumiaux, C., Warny, S., Bellas, S., Gorini, C., Bache, F., Rabineau, M., Estrada, F., 2015. New insights on the Sorbas Basin (SE Spain): the onshore reference of the Messinian Salinity Crisis. Mar. Pet. Geol. 66, 71–100.

Cloetingh, S., van der Beek, P.A., van Rees, D., Roep, T.B., Biermann, C., Stephenson, R.A., 1992. Flexural interaction and the dynamics of Neogene extensional basin formation in the Alboran-Betic region. Geo-Mar. Lett. 12, 66–75.
Comas, M., Garcia-Duenas, V., Jurado, M., 1992. Neogene tectonic evolution of the Alboran Sea from MCS data. Geo-Mar. Lett. 12, 157–164.
Conesa, G., Saint Martin, J.P., Cornee, J.J., Muller, J., 1999. Nouvelles contraintes sur la crise de salinité messinienne par l'étude d'une plate-forme carbonatée marginale (bassin de Sorbas, Espagne). C. R. Acad. Sci. 328, 81–87 (in French).
Corbi, H., Lancis, C., Garcia-Garcia, F., Pina, J.A., Soria, J.M., Tent-Manclus, J.E., Viseras, C., 2012. Updating the marine biostratigraphy of the Granada Basin (central Betic Cordillera). Insight for the Late Miocene palaeogeographic evolution of the Atlantic – Mediterranean seaway. Geobios 45, 249–263.
Cornée, J.J., Saint-Martin, J.P., Conesa, G., Münch, P., André, J.P., Saint-Martin, S., Roger, S., 2004. Correlations and sequence stratigraphic model for Messinian carbonate platforms of the western and central Mediterranean. Int. J. Earth Sci. 93, 621–633.
Cornée, J.J., Münch, P., Achalhi, M., Merzeraud, G., Azdimousa, A., Quillévéré, F., MelinteDobrinescu, M., Chaix, C., Ben Moussa, A., Lofi, J., Séranne, M., Moissette, P., 2016. The Messinian erosional surface and early Pliocene reflooding in the Alboran Sea: new insights from the Boudinar basin, Morocco. Sediment. Geol. 333, 115–129.
Corner, G.D., Nordahl, E., Munch-Ellingsen, K., Robertsen, K.R., 1990. Morphology and sedimentology of an emergent fjord-head Gilbert-type delta: Alta delta, Norway. In:
Colella, A., Prior, D. (Eds.), Coarse-Grained Deltas. IAS Special Publication. 10. Blackwell Science Inc, Oxford, pp. 153–168.
Cosentino, D., Cipollari, P., Mastro, S.L., Giampaolo, C., 2005. High-frequency cyclicity in the latest Messinian Adriatic foreland basin: insight into palaeoclimate and palaeoenvironments of the Mediterranean Lago-Mare episode. Sediment. Geol. 178, 31–53.
Court, W.M., Paul, A., Lokier, S.W., 2017. The preservation potential of environmentally diagnostic sedimentary structures from a coastal sabkha. Mar. Geol. 386, 1–18.
De Decker, P., Chivas, A.R., Shelley, J.M.G., 1988. Paleoenvironments of the Messinian Mediterranean "Lago Mare" from strontium and magnesium in ostracod shells. Palaios 3, 352–358. de Galdeano, C.S., 1990. Geologic evolution of the Betic Cordilleras in the Western Mediterranean, Miocene to the present. Tectonophysics 172, 107–119.
de Galdeano, C.S., Vera, J.A., 1992. Stratigraphic record and palaeogeographical context of the Neogene basins in the Betic Cordillera, Spain. Basin Res. 4, 21–36.
Dercourt, J., Zonenshain, L.P., Ricou, L.E., Kazmin, V.G., Le Pichon, X., Knipper, A.L., Grandjacquet, C., Shotshikov, I.M., Geyssant, J., Lepvrier, C., Perchersky, D.H., Boulin, J., Sibuet, J.C., Savostin, L.A., Sorokhtin, O., Westphal, M., Bazhenov, M.L., Lauer, J.P., Bijou-Duval, B., 1986. Geological evolution of the Tethys belt from the Atlantic to the Pamirs since the Lias. Tectonophysics 123, 241–315.
Dinarès-Turell, J., Sprovieri, R., Caruso, A., Di Stefano, E., Gomis-Coll, E., Pueyo, J.J., Rouchy, J.M., Taberner, C., 1997. Preliminary integrated magnetostratigraphic and biostratigraphic correlation in the Miocene Lorca Basin, (Murcia, SE Spain). Acta Geol. Hisp. 32, 131–170.
Do Couto, D., Gumiaux, C., Augier, R., Lebret, N., Folcher, N., Jouannic, G., Jolivet, L., Suc, J.P., Gorini, C., 2014. Tectonics inversion of an asymmetric graben: Insights from a combined field and gravity survey in the Sorbas basin. Tectonics 33, 1360–1385.
Do Couto, D., Gumiaux, C., Jolivet, L., Augier, R., Lebret, N., Folcher, N., Jouannic, G., Suc, J.P., Gorini, C., 2015. 3D modelling of the Sorbas Basin (Spain): New constraints on the Messinian Erosional Surface morphology. Mar. Pet. Geol. 66, 101–116.
Do Couto, D., Gorini, C., Jolivet, L., Lebret, N., Augier, R., Gumiaux, C., d'Acremont, E., Ammar, A., Jabour, H., Auxietre, J.L., 2016. Tectonic and stratigraphic evolution of the Western Alboran Sea Basin in the last 25 Myrs. Tectonophysics 677–678, 280–311.
Duggen, S., Hoernle, K., Van Den Bogaard, P., Rüpke, L., Morgan, J.P., 2003. Deep roots of the Messinian salinity crisis. Nature 422, 602.
Emery, D., Myers, K.J., 1996. Sequence Stratigraphy. Blackwell Science, Oxford.
Fernandez, J., Bluck, B.J., Viseras, C., 1993. The effects of fluctuating base level on the structure of alluvial fan and associated fan delta deposits: an example from the Tertiary of the Betic Cordillera, Spain. Sedimentology 40, 879–893.
Fortuin, A.R., Dabrio, C., 2008. Evidence for Late Messinian seismites, Nijar Basin, southeast Spain. Sedimentology 55, 1595–1622.
Fortuin, A.R., Krijgsman, W., 2003. The Messinian of the Nijar Basin (SE Spain): sedimentation, depositional environments and paleogeographic evolution. Sediment. Geol. 160, 213–242.
Franseen, E., Mankiewicz, C., 1991. Depositional sequences and correlation of middle(?) to late Miocene carbonate complexes, Las Negras and Nijar areas, southeastern Spain. Sedimentology 38, 871–898.
Frizon de Lamotte, D., Guézou, J.C., Albertini, M.A., 1989. Deformation related to Miocene westward translation in the core of the Betic zone Implications on the tectonic interpretation of the Betic orogen (Spain). Geodin. Acta 3, 267–281.
Galindo-Zaldivar, J., Gonzalez-Lodeiro, F., Jabaloy, A., 1993. Stress and paleaostress in the Betic-rif cordilleras (Miocene to the present). Tectonophysics 227, 105–126.
Garces, M., Krijgsman, W., Agusti, J., 2001. Chronostratigraphic framework and evolution of the Fortuna basin (Eastern Betics) since the Late Miocene. Basin Res. 13, 199–216.
Garcia-Castellanos, D., Estrada, F., Jiménez-Munt, I., Gorini, C., Fernandez, M., Vergés, J., De Vicente, R., 2009. Catastrophic flood of the Mediterranean after the Messinian salinity crisis. Nature 462, 778.
Garcia-Castellanos, D., Micallef, A., Estrada, F., Camerlenghi, A., Ercilla, G., Periáñez, R., Abril, J. M., 2020. The Zanclean megaflood of the Mediterranean–Searching for independent evidence. Earth Sci. Rev. 201. https://doi.org/10.1016/j.earscirev.2019.103061.
Garcia-Garcia, F., Fernandez, J., Viseras, C., Soria, J.M., 2006a. Architecture and sedimentary facies evolution in a delta stack controlled by fault growth (Betic Cordillera, southern Spain, late Tortonian). Sediment. Geol. 185, 79–92.
Garcia-Garcia, F., Fernandez, J., Viseras, C., Soria, J.M., 2006b. High frequency cyclicity in a vertical alternation of Gilbert-type deltas and carbonate bioconstructions in the late Tortonian, Tabernas basin, Southern Spain. Sediment. Geol. 192, 123–139.
Garcia-Veigas, J., Orti, F., Rosell, L., Ingles, M., 1994. Caracterizacion petrologica y geoquimica de la unidad salina messiniense de la cuenca de Lorca (sondeos S4 y S5). Geogaceta 15, 78–81 (in Spanish).
Garcia-Veigas, J., Orti, F., Rosell, L., Ayora, C., Rouchy, J.M., Lugli, S., 1995. The Messinian salt of the Mediterranean: geochemical study of the salt from the Central Sicily Basin and comparison with the Lorca Basin (Spain). Bull. Soc. Geol. Fr. 166, 699–710.
Garcia-Veigas, J., Gibert, L., Cendon, D.I., Artiaga, D., Corbi, H., Soria, J.M., Lowenstein, T.K., Sanz, E., 2019. Late Miocene evaporite geochemistry of Lorca and Fortuna basins (Eastern Betics, SE Spain): Evidences of restriction and continentalization. Basin Res. https://doi.org/10.1111/bre.12408.
Gautier, F., Clauzon, G., Suc, J.P., Cravatte, J., Violanti, D., 1994. Age and duration of the Messinian salinity crisis. C. R. Acad. Sci. 318, 1103–1109.
Ghinassi, M., 2007. The effects of differential subsidence and coastal topography on highorder transgressive–regressive cycles: Pliocene nearshore deposits of the Val d'Orcia Basin, Northern Apennines, Italy. Sediment. Geol. 202, 677–701.
Giaconia, F., Booth-Rea, G., Martinez-Martinez, J.M., Azanon, J.M., Storti, F., Artoni, A., 2014. Heterogeneous extension and the role of transfert faults in the development of the southeastern Betic basins (SE Spain). Tectonics 33, 2467–2489.
Giaconia, F., Booth-Rea, G., Ranero, C.R., Gràcia, E., Bartolome, R., Calahorrano, A., Lo Iacono, C., Vendrell, M., Cameselle, A., Costa, S., Gomez de la Peña, L., MartinezLoriente, S., Perea, H., Viñas, M., 2015. Compressional tectonic inversion of the Algero-Balearic basin: latemost Miocene to present oblique convergence at the Palomares margin (Western Mediterranean). Tectonics 34, 1516–1543.
Gradstein, F.M., Ogg, J.G., Schmitz, M., Ogg, G., 2012. The Geologic Time Scale. 2012.
Elsevier.
Guillen Mondejar, F., Rodriguez Estrella, T., Arana, R., Lopez Aguayo, F., 1995. Historia geologica de la cuenca de Lorca (Murcia): influencia de la tectonica en la sedimentacion. Geogaceta 18, 30–33 (In Spanish).
Gupta, S., Underhill, J., Sharp, I., Gawthorpe, R., 1999. Role of fault interactions in controlling synrift sediment dispersal patterns: Miocene, Abu Alaqa Group, Suez Rift, Sinai, Egypt. Basin Res. 11, 167–189.
Hampton, B., Horton, B., 2007. Sheetflow fluvial processes in a rapidly subsiding basin, Altiplano plateau, Bolivia. Sedimentology 54, 1121–1147.
Haq, B.U., Hardenbol, J., Vail, P., 1987. Chronology of fluctuating sea levels since the Triassic. Science 235, 1156–1167.
Hardie, L., Lowenstein, T., 2004. Did the Mediterranean Sea dry out during the Miocene? A reassessment of the evaporite evidence from DSDP Legs 13 and 42A cores. J. Sediment. Res. 74, 453–461.
Hilgen, F.J., Krijgsman, W., 1999. Cyclostratigraphy and astrochronology of the Tripoli diatomite formation pre-evaporite Messinian, Sicily, Italy. Terra Nova 11, 16–22.
Hilgen, F.J., Krijgsman, W., Langereis, C.G., Lourens, L.J., Santarelli, A., Zachariasse, W.J., 1995. Extending the astronomical (polarity) time scale into the Miocene. Earth Planet. Sci. Lett. 136, 495–510.

Hilgen, F.J., Iaccarino, S., Krijgsman, W., Villa, G., Langereis, C.G., Zachariasse, W.J., 2000a. The global boundary stratotype section and point (GSSP) of the Messinian Stage (uppermost Miocene). Episodes 23, 172–178.

Hilgen, F.J., Bissoli, I., Iaccarino, S., Krijgsman, W., Meijer, R., Negri, A., Villa, G., 2000b. Integrated stratigraphy and astrochronology of the Messinian GSSP at Oued Akrech (Atlantic Morocco). Earth Planet. Sci. Lett. 182, 237–251.

Hilgen, F., Kuiper, K., Krijgsman, W., Snel, E., Van der Laan, E., 2007. Astronomical tuning as the basis for high resolution chronostratigraphy: the intricate history of the Messinian Salinity Crisis. Stratigraphy 4, 231–238.

Horton, B., Schmitt, J.G., 1996. Sedimentology of a lacustrine fan-delta system, Miocene Horse camp Formation, Nevada, USA. Sedimentology 43, 133–155.

Hsü, K.J., 1973. The desiccated deep-basin model for Messinian events. In: Drooger, C.W. (Ed.), Messinian Events in the Mediterranean. North-Holland Publishing Company, Amsterdam, pp. 60–67.

Hsü, K.J., Cita, M.B., Ryan, W.B.F., 1973. The origin of the Mediterranean evaporites. Initial reports DSDP, Washington. 11, pp. 1203–1231.

Huibregtse, P., van Alebeek, H., Zaal, M., Biermann, C., 1998. Palaeostress analysis of the northern Nijar and southern Vera basins: constrains for the Neogene displacement history of major strike-slip faults in the Betic Cordilleras, SE Spain. Tectonophysics 300, 79–101.

Hunt, D., Tucker, M.E., 1992. Stranded parasequences and the forced regressive wedge systems tract: deposition during base-level fall. Sediment. Geol. 81, 1–9.

Hüsing, S.K., Oms, O., Agusti, J., Garcés, M., Kouwenhoven, T., Krijgsman, W., Zachariasse, W.J., 2010. On the late Miocene closure of the Mediterranean–Atlantic gateway through the Guadix basin (southern Spain). Palaeogeogr. Palaeoclimatol. Palaeoecol. 291, 167–179.

Iribarren, L., Verges, J., Camurri, F., Fullea, J., Fernandez, M., 2007. The structure of the Atlantic-Mediterranean transition zone from the Alboran Sea to the Horseshoe abyssal Plain (Iberia-Africa plate boundary). Mar. Geol. 243, 97–119.

Iribarren, L., Verges, J., Fernandez, M., 2009. Sediment supply from the Betic-Rif orogeny to basin through Neogene. Tectonophysics 475, 68–84.

Johnson, C., Franseen, E., Goldstein, R., 2005. The effects of sea level and palaeotopography on lithofacies distribution and geometries in heterozoan carbonates, south-eastern Spain. Sedimentology 52, 513–536.

Jolivet, L., Augier, R., Robin, C., Suc, J.P., Rouchy, J.M., 2006. Lithospheric-scale geodynamic context of the Messinian salinity crisis. Sediment. Geol. 188–189, 9–33.

Jurkschat, T., Fenner, J., Fischer, R., Michalzik, D., 2000. Environmental changes in preevaporitic Late Miocene time in the Lorca Basin (SE Spain): diatom results. In: Hart, M. (Ed.), Climates: Past and Present. 181. Geological Society, London, Special Publications, pp. 65–78.

Karakitsios, V., Roveri, M., Lugli, S., Manzi, V., Gennari, R., Antonarakou, A., Triantaphyllou, M., Agiadi, K., Kontakiotis, G., Kafousia, N., de Rafelis, M., 2017. A record of the Messinian salinity crisis in the eastern Ionian tectonically active domain (Greece, eastern Mediterranean). Basin Res. 29, 203–233.

Kelly, S.B., Olsen, H.O., 1993. Terminal fans - a review with reference to Devonian examples. Sediment. Geol. 85, 339–374.

Kennett, J.P., Srinivasan, M.S., 1983. Neogene Planktonic Foraminifera: A Phylogenetic Atlas. Hutchinson Ross, Stroudsburg.

Krijgsman, W., Meijer, P., 2008. Depositional environments of the Mediterranean “lower evaporites” of the Messinian salinity crisis: constraints from quantitative analyses. Mar. Geol. 253, 73–81.

Krijgsman, W., Hilgen, F.J., Raffi, I., Sierro, F.J., Wilson, D.S., 1999. Chronology, causes and progression of the Messinian salinity crisis. Nature 400, 652–655.

Krijgsman, W., Garces, M., Agusti, J., Raffi, I., Taberner, C., Zachariasse, W.J., 2000. The ‘Tortonian salinity crisis’ of the eastern Betics (Spain). Earth Planet. Sci. Lett. 181, 497–511.

Krijgsman, W., Leewis, M., Garces, M., Kouwenhoven, T., Kuiper, K., Sierro, F., 2006. Tectonic control for evaporite formation in the Eastern Betics (Tortonian; Spain). Sediment. Geol. 188–189, 155–170.

Lancis, C., Tent-Manclus, J.E., Soria, J.M., Caracuel, J.E., Corbi, H., Dinares-Turell, J., Estevez, A., Yebenes, A., 2010. Nannoplankton biostratigraphic calibration of the evaporitic events in the Neogene Fortuna Basin (SE Spain). Geobios 43, 201–217.

Lirer, F., Foresi, L.M., Iaccarino, S.M., Salvatorini, G., Turco, E., Cosentino, C., Sierro, F.J., Caruso, A., 2019. Mediterranean Neogene planktonic foraminifer biozonation and biochronology. Earth Sci. Rev. 196. https://doi.org/10.1016/j.earscirev.2019.05.013.

Lofi, J., Gorini, C., Berné, S., Clauzon, G., Tadeu Dos Rei, A., Ryan, W., Steckler, M., 2005. Erosional processes and paleo-environmental changes in the western Gulf of Lions (SW France) during the Messinian Salinity Crisis. Mar. Geol. 217, 1–30.

Lourens, L., Hilgen, F., Shackleton, N.J., Laskar, J., Wilson, J., 2004. Orbital tuning calibrations and conversionsfor the Neogene Period. In: Gradstein, F.M., Ogg, J.G., Smith, A. G. (Eds.), A Geologic Time Scale 2004. Cambridge University Press, pp. 469–471.

Lugli, S., Manzi, V., Roveri, M., Schreiber, C., 2015. The deep record of the Messinian salinity crisis: evidence of a non-desiccated Mediterranean Sea. Palaeogeogr. Palaeoclimatol. Palaeoecol. 433, 201–218.

Mack, G., James, W., Monger, H., 1993. Classification of paleosols. Geol. Soc. Am. Bull. 105, 129–136.

Madof, A., Bertoni, C., Lofi, J., 2019. Discovery of vast fluvial deposits provides evidence for drawdown during the late Miocene Messinian salinity crisis. Geology 47, 171–174.

Maillard, A., Mauffret, A., 2006. Relationship between erosion surfaces and Late Miocene Salinity Crisis deposits in the Valencia Basin (northwestern Mediterranean): evidence for an early sea-level fall. Terra Nova 18, 321–329.

Maillard, A., Gorini, C., Mauffret, A., Sage, F., Lofi, J., Gaullier, V., 2006. Offshore evidence of polyphase erosion in the Valencia Basin (Northwestern Mediterranean): scenario for the Messinian Salinity Crisis. Sediment. Geol. 188–189, 69–91.

Manzi, V., Gennari, R., Hilgen, F., Krijgsman, W., Lugli, S., Roveri, M., Sierro, F., 2013. Age refinement of the Messinian salinity crisis onset in the Mediterranean. Terra Nova 25, 315–322.

Martin, J.M., Braga, J.C., 1996. Tectonic signals in the Messinian stratigraphy of the Sorbas basin (Almeria, SE Spain). In: Friend, P.F., Dabrio, C. (Eds.), Tertiary Basins of Spain: The Stratigraphic Record of Crustal Kinematics. Cambridge University Press, NewYork, pp. 387–391.

Martin, J.M., Braga, J.C., Sanchez-Almazo, I., 1999. The Messinian record of the outcropping marginal Alboran Basin deposits: significance and implications. Proceedings of the Ocean Drilling Program, Scientific Results. 61, pp. 543–551.

Martin, J.M., Braga, J.C., Sanchez-Almazo, I., Aguirre, J., 2010. Temperate and tropical carbonate-sedimentation episodes in the Neogene Betic basins (southern Spain) linked to climatic oscillations and changes in Atlantic-Mediterranean connections: constraints from isotopic data. In: Mutti, M., Piller, W., Betzler, C. (Eds.), Carbonate Systems during the Oligocene–Miocene Climatic Transition. IAS Special Publications. 42. Willey-Blackwell, Hoboken, pp. 49–70.

Martinez-Diaz, J., 2002. Stress field variation related to fault interaction in a reverse oblique-slip fault: the Alhama de Murcia fault, Betic Cordillera, Spain. Tectonophysics 356, 291–305.

Martinez-Martinez, J., Booth-Rea, G., Azanon, J.M., Torcal, F., 2006. Active transfert fault zone linking a segmented extensional system (Betics, southern Spain): Insight into heterogeneous extension driven by edge delamination. Tectonophysics 422, 159–173.

Marzocchi, A., Flecker, R., Van Baak, C., Lunt, D., Krijgsman, W., 2016. Mediterranean outflow pump: an alternative mechanism for the Lago-mare and the end of the Messinian Salinity Crisis. Geology 44, 523–526.

Massari, F., Parea, G., 1990. Wave-dominated Gilbert-type gravel deltas in the hinterland of the Gulf of Taranto (Pleistocene, southern Italy). In: Colella, A., Prior, D. (Eds.), Coarse Grained Deltas. IAS Special Publication. 10. Blackwell Science Inc, Oxford, pp. 311–331.

McConnico, T., Bassett, K., 2007. Gravelly Gilbert-type fan delta on the Conway Coast, New Zealand: Foreset depositional processes and clast imbrications. Sediment. Geol. 198, 147–166.

McPherson, J., 1980. Genesis of variegated redbeds in the fluvial Aztec siltstone (Late Devonian), southern Victoria Land, Antarctica. Sediment. Geol. 27, 119–142.

Meijninger, B.M.L., Vissers, R.L.M., 2006. Miocene extensional basin development in the Betic Cordillera, SE Spain revealed through analysis of the Alhama de Murcia and Crevillente Faults. Basin Res. 18, 547–571.

Melchor, R., Genise, J., Buatois, L., Umazano, A., 2012. Fluvial environments. In: Knaust, D., Bromley, R.G. (Eds.), Trace Fossils as Indicators of Sedimentary Environments. Developments in Sedimentology. 64. Elsevier, Amsterdam, pp. 329–378.

Merzeraud, G., Achalhi, M., Cornée, J.J., Münch, P., Azdimousa, A., Ben Moussa, A., 2019. Sedimentology and sequence stratigraphy of the late-Messinian – Early Pliocene continental to marine deposits of the Boudinar basin (North Morocco). J. Afr. Earth Sci. 150, 205–223.

Miall, A., 2006. The geology of fluvial deposits. Sedimentary Facies, Basin Analysis, and Petroleum Geology. Springer-Verlag, Berlin-Heidelberg.

Miller, K., Mountain, G., Wright, J., Browning, J., 2011. A 180-million-year record of sea level and ice volume variations from continental margin and deep-sea isotopic records. Oceanography 24, 40–53.

Montenat, C., 1996. The Betic Neogene basins: introduction. In: Friend, P.F., Dabrio, C. (Eds.), Tertiary Basins of Spain: The Stratigraphic Record of Crustal Kinematics. Cambridge University Press, New-York, pp. 321–322.

Montenat, C., Ott d'Estevou, P., 1996. Late Neogene basins evolving in the Eastern Betic transcurrent fault zone: an illustrated review. In: Friend, P.F., Dabrio, C. (Eds.), Tertiary Basins of Spain: The Stratigraphic Record of Crustal Kinematics. Cambridge University Press, New-York, pp. 372–386.

Montenat, C., Ott d'Estevou, P., 1999. The diversity of Late Neogene sedimentary basins generated by wrench faulting in the eastern Betic cordillera, SE Spain. J. Pet. Geol. 22, 61–80.

Mortimer, E., Gupta, S., Cowie, P., 2005. Clinoform nucleation and growth in coarsegrained deltas, Loreto basin, Baja California Sur, Mexico: a response to episodic accelerations in fault displacement. Basin Res. 17, 337–359.

Mulder, T., Syvitski, J.P., Migeon, S., Faugeres, J.C., Savoye, B., 2003. Marine hyperpycnal flows: initiation, behavior and related deposits. A review. Mar. Pet. Geol. 20, 861–882.

Nemec, W., 1990. Aspects of sediment movements on steep delta slopes. In: Colella, A., Prior, D. (Eds.), Coarse Grained Deltas. IAS Special Publication. 10. Blackwell Science Inc, Oxford, pp. 29–73.

Nemec, W., Postma, G., 1993. Quaternary alluvial fans in southewestern Crete: sedimentation processes and geomorphic evolution. In: Marzo, M., Puigdefábregas, C. (Eds.), Alluvial Sedimentation. IAS Special Publication 17. Blackwell, Oxford, pp. 235–276.

Nemec, W., Steel, R.J., 1984. Alluvial and coastal conglomerates: their significant features and some comments on gravelly mass-flow deposits. In: Koster, E.H., Steel, R.J. (Eds.), Sedimentology of Gravels and Conglomerates. Memoirs of the Canadian Society of Petroleum Geology, Calgary, pp. 1–30.

Omodeo-Salé, S., Gennari, R., Lugli, S., Manzi, V., Roveri, M., 2012. Tectonic and climatic control on the Late Messinian sedimentary evolution of the Nijar Basin (Betic Cordillera, Southern Spain). Basin Res. 24, 314–337.

Orszag-Sperber, F., 2006. Changing perspectives in the concept of "Lago-Mare" in Mediterranean Late Miocene evolution. Sediment. Geol. 188, 259–277.

Orszag-Sperber, F., Plaziat, J.C., Baltzer, F., Purser, B.H., 2001. Gypsum salina–coral reef relationships during the Last Interglacial (marine isotopic stage 5e) on the Egyptian Red Sea coast: a Quaternary analogue for Neogene marginal evaporites? Sediment. Geol. 140, 61–85.

Orszag-Sperber, F., Caruso, A., Blanc-Valleron, M.M., Merle, D., Rouchy, J.M., 2009. The onset of the Messinian salinity crisis: Insights from the Cyprus sections. Sediment. Geol. 217, 52–64.

Orti, F., Garcia-Veigas, J., Rosell, L., Rouchy, J.M., Inglés, M., Gimeno, D., Kasprzyk, A., Playa, E., 1993. Correlacion litoestratigrafica de las evaporitas mesinienses en las cuencas de Lorca y Fortuna (Murcia). Geogaceta 14, 98–101 (in Spanish).

Orton, G.J., Reading, H., 1993. Variability of deltaic processes in terms of sediment supply, with particular emphasis on grain size. Sedimentology 40, 475–512.

Pedrera, A., Marin-Lechado, C., Galindo-Zaldivar, J., Rodriguez-Fernandez, L.R., RuizConstan, A., 2006. Fault and fold interaction during the development of the Neogene-Quaternary Almeria-Nijar basin (SE Betic Cordilleras). In: Moratti, G., Chalouan, A. (Eds.), Tectonics of the Western Mediterranean and North Africa. Special Publications, London, Geological Society of London, pp. 217–230.

Pellegrino, L., Pierre, F., Natalicchio, M., Carnevale, G., 2018. The Messinian diatomite deposition in the Mediterranean region and its relationships to the global silica cycle. Earth Sci. Rev. 178, 154–176.

Perch-Nielsen, K., 1985. Cenozoic calcareous nannofossils. In: Bolli, H.M., Saunders, J.B., Perch-Nielsen, K. (Eds.), Plankton Stratigraphy. Cambridge University Press, Cambridge, pp. 427–555.

Perrin, C., Bosellini, F.R., 2013. The Late Miocene coldspot of z-coral diversity in the Mediterranean: patterns and causes. CR Palevol 12, 245–255.

Pierre, C., Caruso, A., Blanc-Valleron, M.-M., Rouchy, J.M., Orzsag-Sperber, F., 2006. Reconstruction of the paleoenvironmental changes around the Miocene–Pliocene boundary along a West–East transect across the Mediterranean. Sediment. Geol. 188–189, 319–340.

Pla-Pueyo, S., Gierlowski-Kordesch, E., Viseras, C., Soria, J., 2009. Major controls on sedimentation during the evolution of a continental basin: Pliocene–Pleistocene of the Guadix Basin (Betic Cordillera, southern Spain). Sediment. Geol. 219, 97–114.

Platt, J.P., 2007. From orogenic hinterlands to Mediterranean-style back-arc basins: a comparative analysis. J. Geol. Soc. Lond. 164, 297–311.

Playà, E., Orti, F., Rosell, L., 2000. Marine to non-marine sedimentation in the upper Miocene evaporites of the Eastern Betics, SE Spain: sedimentological and geochemical evidence. Sediment. Geol. 133, 135–166.

Plint, A.G., Nummedal, D., 2000. The falling stage systems tract: recognition and importance in sequence stratigraphic analysis. In: Hunt, D., Gawthorpe, R.L. (Eds.), Sedimentary Responses to Forced Regressions. Special Publication, London, Geological Society of London, pp. 1–17.

Popescu, S.M., Dalibard, M., Suc, J.P., Barhoun, N., Melinte-Dobrinescu, M.C., Bassetti, M., Deaconu, F., Head, M., Gorini, C., Do Couto, D., Rubino, J.L., Auxietre, J.L., Floodpage, J., 2015. Lago Mare episodes around the Messinian–Zanclean boundary in the deep southwestern Mediterranean. Mar. Pet. Geol. 66, 55–70.

Posamentier, H.W., Allen, G.P., 1999. Siliciclastic Sequence Stratigraphy: Concepts and Applications. SEPM Concepts in Sedimentology and Paleontology 7, Tulsa.

Postma, G., 1990. Depositional architecture and facies of river and fan deltas: a synthesis. In: Colella, A., Prior, D. (Eds.), Coarse Grained Deltas, IAS Special Publication 10. Blackwell Science Inc, Oxford, pp. 13–27.

Postma, G., Nemec, W., Kleinspehn, K., 1988. Large floating clasts in turbidites: a mechanism for their emplacement. Sediment. Geol. 58, 47–61.

Prior, D., Bornhold, B., 1989. Submarine sedimentation on a developing Holocene fan delta. Sedimentology 36, 1053–1076.

Prior, D., Bornhold, B., 1990. The underwater development of Holocene fan deltas. In: Colella, A., Prior, D. (Eds.), Coarse Grained Deltas. IAS Special Publication. 10. Blackwell Science Inc, Oxford, pp. 75–90.

Raffi, I., Mozzato, C.A., Fornaciari, E., Hilgen, F.J., Rio, D., 2003. Late Miocene calcareous nannofossil biostratigraphy and astrobiochronology for the Mediterranean region. Micropaleontology 49, 1–26.

Raffi, I., Backman, J., Fornaciari, E., Pälike, H., Rio, D., Lourens, L., Hilgen, F., 2006. A review of calcareous nannofossil astrobiochronology encompassing the past 25 million years. Quat. Sci. Rev. 25, 3113–3137.

Retallack, G., 1988. Field recognition of paleosols. Geol. Soc. Am. Spec. Pap. 216, 1–20.

Riaza, C., Martinez del Olmo, W., 1996. Depositional model of the Guadalquivir-Gulf of Cadiz Tertiary basin. In: Friend, P.F., Dabrio, C. (Eds.), Tertiary Basins of Spain: The Stratigraphic Record of Crustal Kinematics. Cambridge University Press, New-York, pp. 330–338.

Ridgway, K., Decelles, P., 1993. Stream-dominated alluvial fan and lacustrine depositional systems in Cenozoic strike-slip basins, Denali fault system, Yukon Territory, Canada. Sedimentology 40, 645–666.

Riding, R., Braga, J.C., Martin, J.M., Sánchez-Almazo, I.M., 1998. Mediterranean Messinian Salinity Crisis: constraints from a coeval marginal basin, Sorbas, southeastern Spain. Mar. Geol. 146, 1–20.

Rodríguez-Fernández, J., de Galdeano, C.S., 2006. Late orogenic intramontane basin development: the Granada basin, Betics (southern Spain). Basin Res. 18, 85–102.

Rodriguez-Fernandez, J., Azor, A., Azanon, J.M., 2012. The Betic intramontane basins (SE Spain): stratigraphy, subsidence, and tectonic history. In: Busby, C., Azor, A. (Eds.), Tectonics of Sedimentary Basins: Recent Advances. Blackwell Publishing, Oxford, pp. 461–479.

Roep, T., Dabrio, C., Fortuin, A., Polo, M., 1998. Late highstand patterns of shifting and stepping coastal barriers and washover-fans (late Messinian, Sorbas Basin, SE Spain). Sediment. Geol. 116, 27–56.

Roger, S., Münch, P., Cornée, J.J., Saint Martin, J.P., Féraud, G., Pestrea, S., Conesa, G., Ben Moussa, A., 2000. $^{40}Ar/^{39}Ar$ dating of the pre-evaporitic Messinian marine sequences of the Melilla basin (Morocco): a proposal for some biosedimentary events as isochrons around the Alboran Sea. Earth Planet. Sci. Lett. 179, 101–113.

Rouchy, J.M., Caruso, A., 2006. The Messinian salinity crisis in the Mediterranean basin: a reassessment of the data and an integrated scenario. Sediment. Geol. 188–189, 35–67.

Rouchy, J.M., Taberner, C., Blanc-Valleron, M.-M., Sprovieri, R., Russell, M., Pierre, C., Di Stefano, E., Pueyo, J.J., Caruso, A., Dinarès-Turell, J., Gomis-Coll, E., Wolff, G.A., Cespuglio, G., Ditchfield, P., Pestrea, S., Combourieu-Nebout, N., Santisteban, C., Grimalt, J.O., 1998. Sedimentary and diagenetic markers of the restriction in a marine basin: the Lorca Basin (SE Spain) during the Messinian. Sediment. Geol. 121, 23–55.

Rouchy, J.M., Orszag-Sperber, F., Blanc-Valleron, M.M., Pierre, C., Rivière, M., CombourieuNebout, N., Panayides, I., 2001. Paleoenvironmental changes at the Messinian–Pliocene boundary in the eastern Mediterranean (southern Cyprus basins): significance of the Messinian Lago-Mare. Sediment. Geol. 145, 93–117.

Roveri, M., Manzi, V., 2006. The Messinian salinity crisis: looking for a new paradigm? Palaeogeogr. Palaeoclimatol. Palaeoecol. 238, 386–398.

Roveri, M., Lugli, S., Manzi, V., Schreiber, B.C., 2008. The Messinian Sicilian stratigraphy revisited: new insights for the Messinian salinity crisis. Terra Nova 20, 483–488.

Roveri, M., Flecker, R., Krijgsman, W., Lofi, J., Lugli, S., Manzi, V., Sierro, F., Bertini, A., Camerlenghi, A., De Lange, G., Govers, R., Hilgen, F., Hübscher, C., Meijer, P., Stoica, M., 2014a. The Messinian Salinity Crisis: past and future of a great challenge for marine sciences. Mar. Geol. 352, 25–58.

Roveri, M., Lugli, S., Manzi, V., Gennari, R., Schreiber, B.C., 2014b. High-resolution strontium isotope stratigraphy of the Messinian deep Mediterranean basins: Implications for marginal to central basins correlation. Mar. Geol. 349, 113–125.

Roveri, M., Gennari, R., Ligi, M., Lugli, S., Manzi, V., Reghizzi, M., 2019. The synthetic seismic expression of the Messinian salinity crisis from onshore records: Implications for shallow-to deep-water correlations. Basin Res. 36, 1121–1152.

Russell, M., Grimalt, J.O., Hartgers, W.A., Taberner, C., Rouchy, J.M., 1997. Bacterial and algal markers in sedimentary organic matter deposited under natural sulphurization conditions (Lorca Basin, Murcia, Spain). Org. Geochem. 26, 605–625.

Ryan, W.B.F., 2009. Decoding the Mediterranean salinity crisis. Sedimentology 56, 95–136.

Saelen, G., Lunde, I.L., Porten, K.W., Braga, J., Dundas, S.H., Ninnemann, U.S., Ronen, Y., Talbot, M.R., 2016. Oyster shells as recorders of short-term oscillations of salinity and temperature during deposition of coral bioherms and reefs in the Miocene Lorca Basin, SE Spain. J. Sediment. Res. 86, 637–667.

Sánchez-Almazo, I., Spiro, B., Braga, J., Martın, J., 2001. Constraints of stable isotope signatures on the depositional palaeoenvironments of upper Miocene reef and temperate carbonates in the Sorbas Basin, SE Spain. Palaeogeogr. Palaeoclimatol. Palaeoecol. 175, 153–172.

Sánchez-Almazo, I., Braga, J., Dinares-Turell, J., Martín, J., Spiro, B., 2007. Palaeoceanographic controls on reef deposition: the Messinian Cariatiz reef (Sorbas Basin, Almería, SE Spain). Sedimentology 54, 637–660.

Santisteban, C., Taberner, C., 1983. Shallow marine and continental conglomerates derived fromcoral reef complexes after desiccation of a deep marine basin: the Tortonian-Messinian deposits of the Fortuna Basin SE, Spain. J. Geol. Soc. Lond. 140, 401–411.

Soria, J., Fernandez, J., Viseras, C., 1999. Late Miocene stratigraphy and palaeogeographic evolution of the intramontane Guadix Basin (Central Betic Cordillera, Spain): implications for an Atlantic–Mediterranean connection. Palaeogeogr. Palaeoclimatol. Palaeoecol. 151, 255–266.

Soria, J., Caracuel, J.E., Yébenes, A., Fernandez, J., Viseras, C., 2005. The stratigraphic record of the Messinian salinity crisis in the northern margin of the Bajo Segura Basin (SE Spain). Sediment. Geol. 179, 225–247.

Soria, J., Caracuel, J.E., Corbi, H., Dinarès-turell, J., Lancis, C., Tent-Manclus, J., Viseras, C., Yébenes, A., 2008. The Messinian–early Pliocene stratigraphic record in the southern Bajo Segura Basin (Betic Cordillera, Spain): Implications for the Mediterranean salinity crisis. Sediment. Geol. 203, 267–288.

Sprovieri, R., Di Stefano, E., Sprovieri, M., 1996. High resolution chronology for late Miocene Mediterranean stratigraphic events. Riv. Ital. Paleontol. Stratigr. 102, 77–104.

Stanistreet, I., McCarthy, T., 1993. The Okavango Fan and the classification of subaerial fan systems. Sediment. Geol. 85, 115–133.

Steel, E., Simms, A.R., Steel, R., Olariu, C., 2018. Hyperpycnal delivery of sand to the continental shelf: Insights from the Jurassic Lajas Formation, Neuquén Basin, Argentina. Sedimentology 65, 2149–2170.

Stefano, L., Vinicio, M., Marco, R., Charlotte, S.B., 2010. The primary lower Gypsum in the Mediterranean: a new facies interpretation for the first stage of the Messinian salinity crisis. Palaeogeogr. Palaeoclimatol. Palaeoecol. 297, 83–99.

Stoica, M., Krijgsman, W., Fortuin, A., Gliozzi, E., 2016. Paratethyan ostracods in the Spanish Lago-Mare: more evidence for interbasinal exchange at high Mediterranean sealevel. Palaeogeogr. Palaeoclimatol. Palaeoecol. 441, 854–870.

Stow, D., Shanmugam, G., 1980. Sequence of structures in fine-grained turbidites: comparison of recent deep-sea and ancient flysch sediments. Sediment. Geol. 25, 23–42.

Tent-Manclus, J., Soria, J., Estevez, A., Lancis, C., Caracuel, J., Dinarès-Turell, J., Yébenes, A., 2008. The Tortonian salinity crisis in the Fortuna Basin (southeastern Spain): Stratigraphic record, tectonic scenario and chronostratigraphy. C. R. Geosci. 340, 474–481.

Thrana, C., Talbot, M.R., 2006. High-frequency carbonate-siliciclastic cycles in the Miocene of the Lorca Basin (Western Mediterranean, SE Spain). Geol. Acta 4, 343–354.

Urgeles, R., Camerlenghi, A., Garcia-Castellanos, D., De Mol, B., Garcés, M., Vergés, J., Haslam, I., Hardman, M., 2011. New constraints on the Messinian sealevel drawdown from 3D seismic data of the Ebro margin, western Mediterranean. Basin Res. 23, 123–145.

Vazquez, M., Jabaloy, A., Barbero, L., Stuart, F.M., 2011. Deciphering tectonic- and erosiondriven exhumation of the Nevado-Filabride complex (Betic Cordillera, Southern Spain) by low temperature thermochronology. Terra Nova 23, 257–263.

Vennin, E., Rouchy, J.M., Chaix, C., Blanc-Valleron, M.M., Caruso, A., Rommevau, V., 2004. Paleoecological constraints on reef-coral morphologies in the Tortonian–early Messinian of the Lorca Basin, SE Spain. Palaeogeogr. Palaeoclimatol. Palaeoecol. 213, 163–185.

Vera, J.A., 1983. Las zonas externas de las cordilleras Béticas. Geología de España, Tomo 2. Instituto Geológico Minero de España, Madrid, pp. 218–251 (in Spanish).

Vissers, R., Platt, J., Van der Wal, D., 1995. Late orogenic extension of the Betic Cordillera and the Alboran Domain: a lithospheric view. Tectonics 14, 786–803.

Warren, J.K., 2006. Evaporites: Sediments, Resources and Hydrocarbons. Springer-Verlag, Berlin Heidelberg.

Warrlich, G., Bosence, D., Waltham, D., 2005. 3D and 4D controls on carbonate depositional systems: Sedimentological and sequence stratigraphic analysis of an attached carbonate platform and atoll (Miocene, Nijar Basin, SE Spain). Sedimentology 52, 363–389.

Winsemann, J., Asprion, U., Meyer, T., Schramm, C., 2007. Facies characteristics of Middle Pleistocene (Saalian) ice-margin subaqueous fan and delta deposits, glacial Lake Leine, NW Germany. Sediment. Geol. 193, 105–129.

Winsemann, J., Hornung, J., Meinsen, J., Asprion, U., Polom, U., Brandes, C., Bußmann, M., 2009. Anatomy of a subaqueous ice-contact fan and delta complex, Middle Pleistocene, North-west Germany. Sedimentology 56, 1041–1076.

Wrobel, F., Michalzik, D., 1999. Facies successions in the pre-evaporitic Late Miocene of the Lorca Basin, SE Spain. Sediment. Geol. 127, 171–191.

Young, J.R., 1998. Neogene. In: Bown, P.R. (Ed.), Calcareous Nannofossil Biostratigraphy. British Micropalaeontological Society Publication Series, pp. 225–265.

Zavala, C., Ponce, J.J., Arcuri, M., Drittanti, D., Freije, H., Asensio, M., 2006. Ancient lacustrine hyperpycnites: a depositional model from a case study in the Rayoso Formation (Cretaceous) of west-central Argentina. J. Sediment. Res. 76, 41–59.

Zavala, C., Arcuri, M., Di Meglio, M., Gamero Diaz, H., Contreras, C., 2011. A genetic facies tract for the analysis of sustained hyperpycnal flow deposits. In: Slatt, R.M., Zavala, C. (Eds.), Sediment Transfer from Shelf to Deep Water-Revisiting the Delivery System.
61, pp. 31–51 AAPG Studies in Geology.